

DRAFT

AIRBORNE GEOPHYSICAL ASSESSMENT OF SALINIZATION
IN THE LACY CREEK AREA, STERLING COUNTY, TEXAS

by

Jeffrey G. Paine
Research Scientist
Bureau of Economic Geology
The University of Texas at Austin

Mail address:
University Station, Box X
Austin, Texas 78713-8924

Street address:
J. J. Pickle Research Campus, Building 130
10100 Burnet Road
Austin, Texas 78758-4445

jeff.paine@beg.utexas.edu

Report prepared for the Upper Colorado River Authority
under Contract No. 2000-483-349

January 2002

Page intentionally blank

CONTENTS

SUMMARY	1
INTRODUCTION	2
METHODS	5
Ground Geophysics	6
Airborne Geophysics	7
GROUNDWATER DEPTH	12
GROUNDWATER QUALITY	12
MAGNETIC FIELD DATA	17
AIRBORNE EM DATA	18
Apparent Conductance	19
Conductivity-Depth Slices	21
Conductivity Cross Section	25
Quantifying the Relationship Between Conductivity and Water Salinity	27
Comparison with Ground-Based EM Measurements	29
EXTENT AND INTENSITY OF SALINIZATION	34
CONCLUSIONS	35
ACKNOWLEDGMENTS	36
REFERENCES	37
APPENDIX: CONDUCTIVITY-DEPTH SLICES BETWEEN 10 AND 200-M DEPTH	39

FIGURES

1. Location of the airborne survey area in central Sterling County, Texas	3
2. Locations of oil and gas wells within the airborne survey area	4
3. Aerial photographic mosaic of the airborne survey area and locations of EM lines	6
4. Flight lines flown by Fugro Airborne Surveys	8

5.	Time-domain EM transmitter input and receiver response	8
6.	The DeHavilland Dash-7 used to acquire airborne geophysical data	10
7.	Survey aircraft acquiring TDEM and magnetic field data	10
8.	Location and water depths of water wells in the airborne survey area	13
9.	Relationship between water depth and surface elevation	13
10.	Relationship between land-surface elevation and water elevation	14
11.	Relationship between total dissolved solids concentration and specific conductivity	15
12.	High, mean, median, and low concentrations of common anions	16
13.	High, mean, median, and low concentrations of common cations	16
14.	Residual magnetic field intensity measured during the airborne survey	18
15.	Powerline noise intensity measured during the airborne survey	20
16.	Apparent conductance calculated from TDEM data	20
17.	Location of the Parochial Bade Oil Field, the Durham Oil Field, and section A–A'	25
18.	Cross section A–A' across the Parochial Bade field	26
19.	Relationship between TDS and apparent conductivities	28
20.	Apparent conductivity acquired using a ground-based conductivity meter	30
A1.	Apparent conductivity at a depth of 10 m	40
A2.	Apparent conductivity at a depth of 20 m	40
A3.	Apparent conductivity at a depth of 30 m	41
A4.	Apparent conductivity at a depth of 40 m	41
A5.	Apparent conductivity at a depth of 50 m	42
A6.	Apparent conductivity at a depth of 60 m	42
A7.	Apparent conductivity at a depth of 70 m	43
A8.	Apparent conductivity at a depth of 80 m	43
A9.	Apparent conductivity at a depth of 90 m	44
A10.	Apparent conductivity at a depth of 100 m	44
A11.	Apparent conductivity at a depth of 110 m	45

A12.	Apparent conductivity at a depth of 120 m	45
A13.	Apparent conductivity at a depth of 130 m	46
A14.	Apparent conductivity at a depth of 140 m	46
A15.	Apparent conductivity at a depth of 150 m	47
A16.	Apparent conductivity at a depth of 160 m	47
A17.	Apparent conductivity at a depth of 170 m	48
A18.	Apparent conductivity at a depth of 180 m	48
A19.	Apparent conductivity at a depth of 190 m	49
A20.	Apparent conductivity at a depth of 200 m	49

TABLES

1.	Types of oil and gas well locations within the airborne survey area	5
2.	Survey and flight parameters for the Sterling County airborne geophysical survey	7
3.	Acquisition parameters for the Sterling County airborne TDEM survey	9
4.	Acquisition parameters for the Sterling County airborne magnetometer survey	12
5.	Salinity classifications based on TDS concentration	15
6.	Wells used to compare water quality and apparent conductivity	22

SUMMARY

In late August and early September 2001, a high-resolution airborne geophysical survey was flown over a 162 km² area west of Sterling City in Sterling County, Texas. This survey, flown to delineate salinization and estimate its intensity in the shallow, relatively fresh groundwater of the alluvial and Antlers aquifers, acquired magnetic field data to aid the identification of oil and gas wells and electromagnetic (EM) induction data to reveal the electrical conductivity of the ground to depths of 150 m or more. We used water well data from the Texas Water Development Board (TWDB) database and oil and gas well locations from the Texas Railroad Commission (RRC) to assess the accuracy and usefulness of the magnetic field and ground conductivity data. Additionally, we collected ground conductivity data along several transects using a ground-based conductivity meter. We used these data to design the airborne survey, anticipate airborne exploration depths, select the appropriate airborne instruments, compare airborne and ground-based measurements over the same area, and investigate evidence for salinization at several representative locations. We combined aerial photographs, oil and gas well data, water well data, and airborne and ground-based geophysical data in a geographic database (GIS) to facilitate analysis of geophysical anomalies and determine the relationship between water properties and geophysical measurements.

The magnetic field data accurately identified most of the more than 400 oil and gas well locations in the survey area. In some cases, magnetic anomaly locations more accurately represented the well locations than did locations obtained from the RRC database. Anomalies associated with some wells located equidistant from adjacent flight lines (spaced at 100 m) were not detected by the airborne instruments. In some places where many wells are densely clustered, the airborne magnetometer identified a single anomaly for a group of closely spaced wells.

Ground conductivity values derived from the airborne EM data are similar to conductivities measured by ground-based instruments. Data obtained from the airborne survey show that the ground beneath the valleys is more electrically conductive than the ground beneath the plateaus,

largely because water depths are shallower in the valleys, Edwards Group limestones capping the plateaus are poorly conductive, and the alluvial sediments and Cretaceous and older strata beneath the valleys are more conductive than the limestones. Apparent conductivities calculated from the airborne geophysical data at 10-m intervals between the depths of 10 to more than 200 m below the ground surface show that conductivities are generally low in the survey area. Low conductivities are consistent with the generally good water quality reported in most of the shallow wells, where water is dominantly fresh to slightly saline. There are local areas of elevated ground conductivity, notably in and near the Parochial Bade Oil Field in the southwestern part of the survey area. Elevated conductivity in this area is associated with abandoned salt-water disposal pits identified in a 1993 RRC report on salt-water contamination in the Parochial Bade field. Conductivity values in another area of concern, the Durham Oil Field located southwest of Sterling City, are relatively low and show little evidence of salinization to depths of 100 m or more.

INTRODUCTION

We conducted airborne and supporting ground-based geophysical studies in Sterling County, Texas (fig. 1) on behalf of the Upper Colorado River Authority (UCRA) and the Texas Water Development Board (TWDB). The purpose of these studies is to examine the intensity of salinization of groundwater in the shallow subsurface (upper few hundred meters). The project area, located west of Sterling City, is a rectangular block covering 162 km² that is about 17.8 km across in an east–west direction and about 9.1 km across in a north–south direction.

The principal geophysical method employed in this study is time-domain electromagnetic induction (TDEM), in which changes in electrical currents flowing in a transmitter wire induce changes in the local magnetic field, which in turn induce currents to flow in the ground beneath the transmitter. The recorded decay of the magnetic field produced by the ground currents contains information about the electrical conductivity of the ground. Electrical conductivity of the

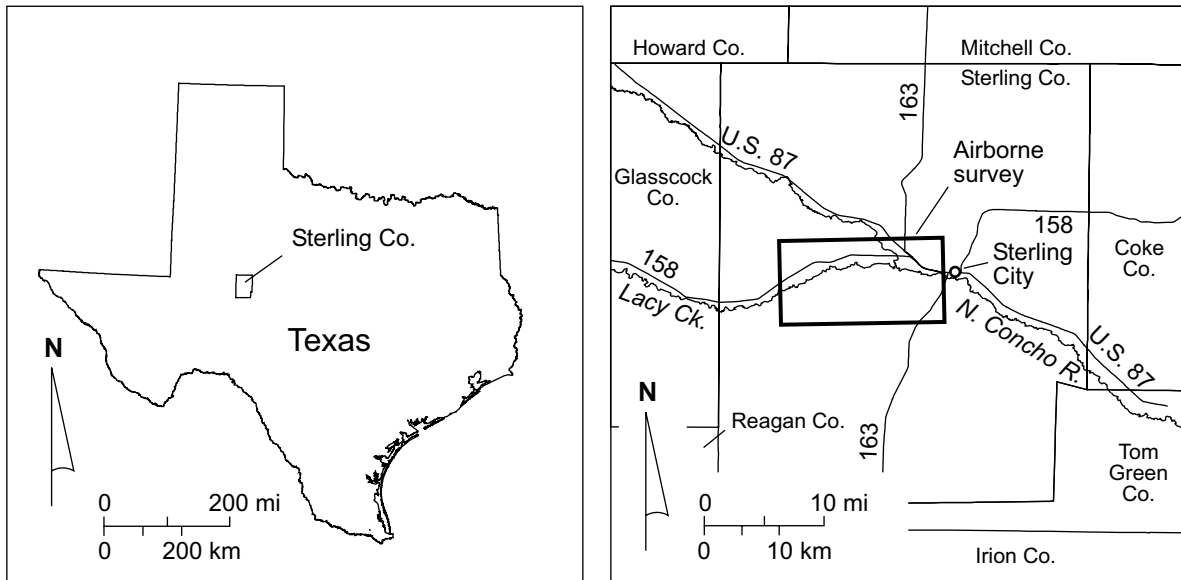


Figure 1. Location of the airborne survey area in central Sterling County, Texas.

ground is influenced both by sediment type (clayey sediments are more conductive than sandy sediments) and by water quality (saline water is more conductive than fresh water). Salinized areas will have relatively high electrical conductivity, whereas nonsalinized areas will have relatively low conductivity. The Sterling County airborne geophysical survey covers an area that is about twice as large as that of the recent Runnels County survey (Paine and others, 1999), uses an instrument that explores to significantly greater depths, and produces images of conductivity at depth.

Dense spatial data were obtained by mounting the geophysical instruments in an aircraft and flying at low altitude on a tight grid over the survey area, allowing potential subsurface changes in water quality to be interpreted. The airborne geophysical data were verified by (1) acquiring ground-based geophysical data at representative locations and comparing ground and airborne results and (2) comparing available water well data to conductivity patterns evident in the airborne data set.

Groundwater quality within the survey area, both from an alluvial aquifer along Lacy Creek and from the Antlers Sand aquifer, is generally good. Local salinization of Antlers groundwater related to oil and gas exploration and production has been documented in the Parochial Bade Oil

Field (Renfro, 1993). We obtained oil and gas well locations within the survey area from the Texas Railroad Commission (RRC) to examine the extent of this salinization and to delineate other areas of potential oilfield salinization. RRC records indicate that there are 475 well locations within the survey area (fig. 2), with the densest concentrations in the Parochial Bade field in the southwest part of the area and in the Durham Oil Field in the southeast part of the area. Of these 475 locations (table 1 and fig. 2), the majority are either producing oil wells (211) or plugged oil wells (109). Less than five percent represent locations where no well exists, either as a permit only (15) or a cancelled or abandoned location (5). There are 12 injection or saltwater disposal wells. Potential oilfield-related salinization could be caused by past discharge of pro-

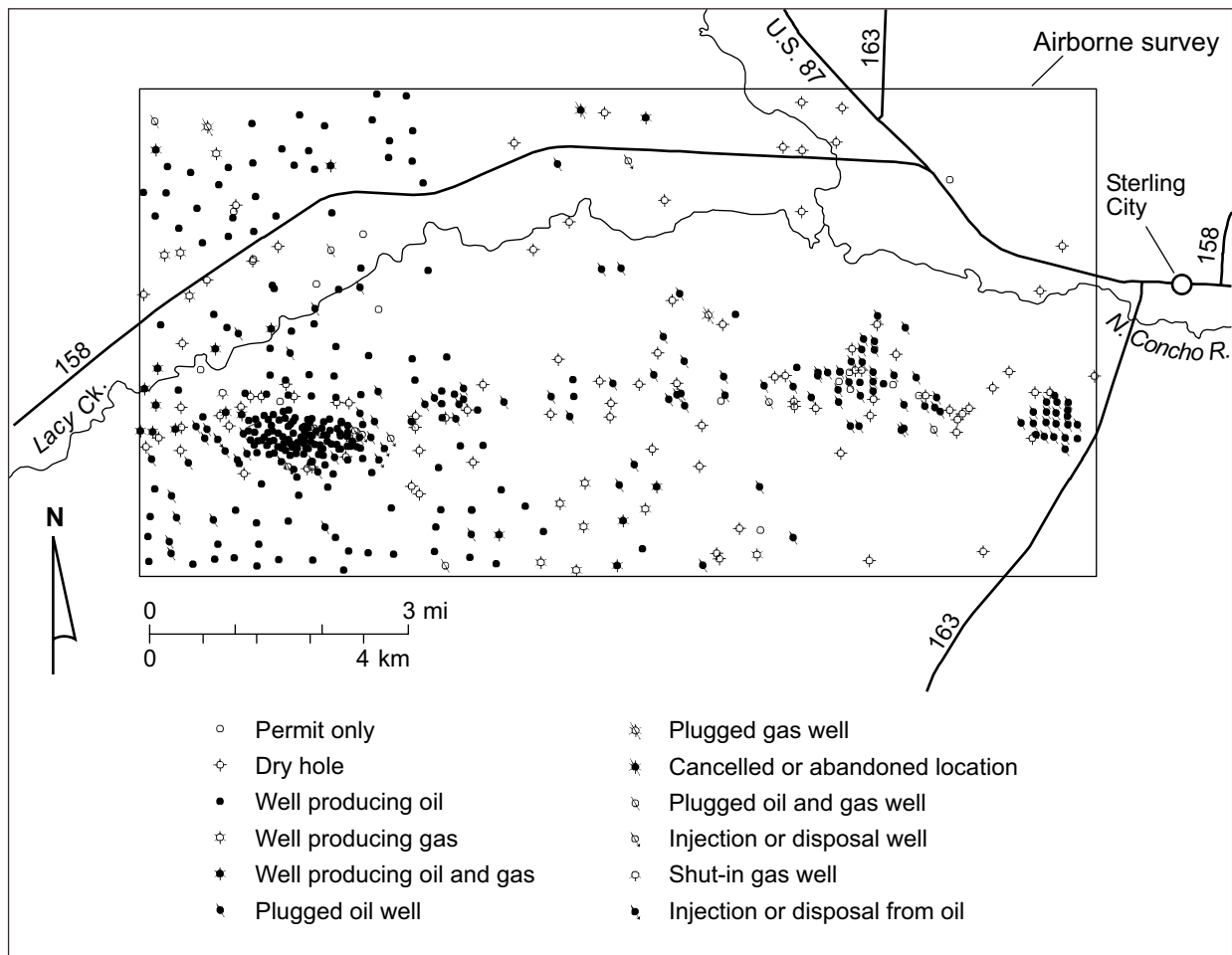


Figure 2. Locations of oil and gas wells within the airborne survey area. Well data from the Texas Railroad Commission (RRC).

Table 1. Types of oil and gas well locations within the airborne survey area, Sterling County, Texas. Data from Texas Railroad Commission. Locations shown on fig. 2.

Permit only (type 2)	15
Dry hole with surface casing (type 3)	91
Well producing oil (type 4)	211
Well producing gas (type 5)	11
Well producing oil and gas (type 6)	17
Plugged oil well (type 7)	109
Plugged gas well (type 8)	2
Cancelled or abandoned location (type 9)	5
Plugged oil and gas well (type 10)	1
Injection or disposal well (type 11)	6
Shut-in gas well (type 20)	1
Injection or disposal from oil (type 21)	6
Total oil and gas well locations	475

duced water into pits, migration of saline water from deeper formations into the shallow aquifers, and leakage of injected saline water into the shallow aquifers. In each of these cases, significant salinization of the shallow aquifers should be accompanied by an increase in electrical conductivity of the ground near the leaking well or pit. Magnetic field data from the airborne geophysical surveys can be used along with known well locations to verify well locations and locate either unknown or mislocated wells. Conductivity data can be used to identify conductivity anomalies consistent with salinization. When combined, these data can help distinguish natural and oilfield sources of salinization (Paine and others, 1999).

METHODS

We employed airborne and ground-based geophysical methods to rapidly and noninvasively delineate potentially salinized areas by measuring changes in electrical conductivity with depth. The principal geophysical method in the airborne and ground surveys is electromagnetic induction, or simply EM (Parasnis, 1973; Frischknecht and others, 1991; West and Macnae, 1991). This family of geophysical methods employs a changing primary magnetic field that is created

around a current-carrying transmitter wire to induce a current to flow within the ground, which in turn creates a secondary magnetic field that is sensed by a receiver coil. In general, the strength of the secondary field is proportional to the conductivity of the ground.

Ground Geophysics

In January 2001, we acquired ground conductivity data west of Sterling City using a Geonics EM34 ground conductivity meter (McNeill, 1980). This instrument measures apparent electrical conductivity of the ground at multiple exploration depths. It consists of transmitter and receiver coils that are connected by a cable and separated by distances of 10-, 20-, and 40-m, depending on the operating frequency and exploration depth desired.

We collected data at either the 20- or 40-m coil separation along nine lines (EM lines A through I, fig. 3). At the 20-m coil separation (1600 Hz operating frequency), exploration depth in the horizontal dipole mode is about 12 m. Exploration depth in the horizontal dipole mode

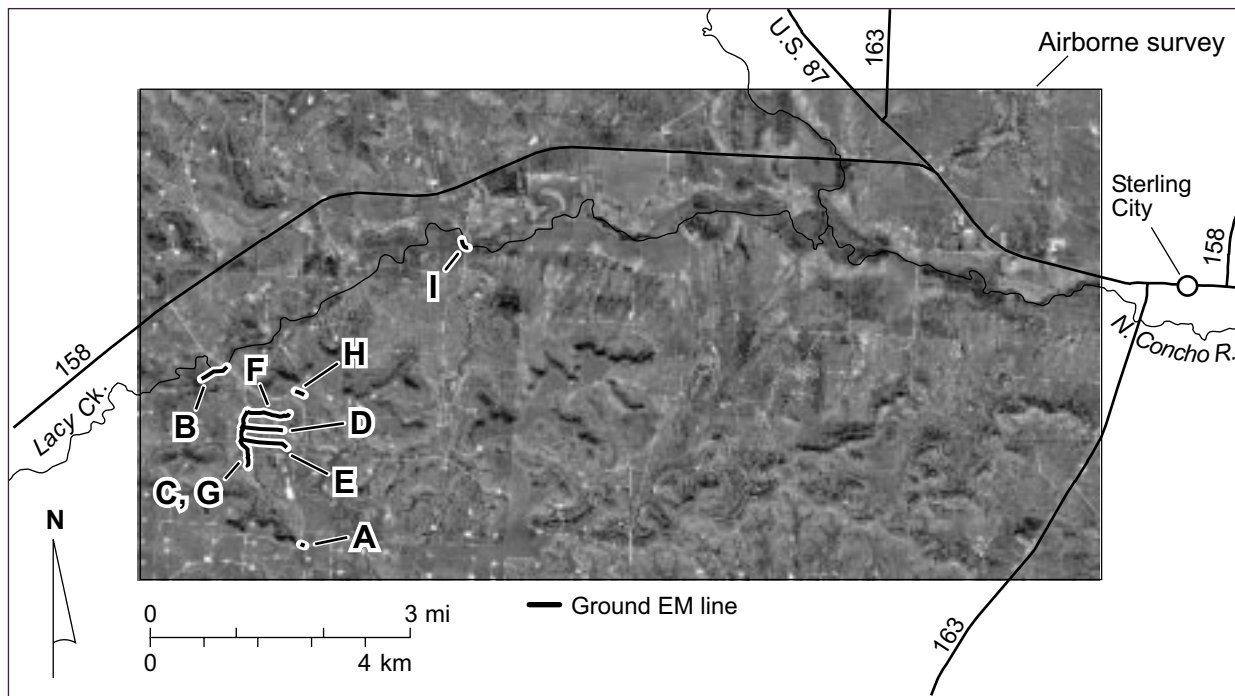


Figure 3. Aerial photographic mosaic of the airborne survey area and locations of EM lines acquired using a ground-based instrument. Aerial photographs taken in January 1996 and modified from digital originals provided by the Texas Natural Resources Information System.

increases to about 24 m at the 40-m coil separation (400 Hz). Deeper exploration can be achieved by orienting the coils in vertical dipole mode (25 m for the 20-m separation and 51 m for the 40-m separation), but metallic objects and power lines typical of oilfield areas commonly make these data unreliable. We used a GPS receiver to locate the ground-based geophysical lines.

Airborne Geophysics

Fugro Airborne Surveys flew an airborne geophysical survey of the study area in late August and early September 2001 (table 2). The survey covered an area of about 162 km² west of Sterling City (fig. 4). The principal flight lines were 9.1 km long, oriented north–south, and spaced 100-m apart. The three tie lines were 17.8 km long, oriented east–west, and spaced 4,000-m apart. A total of 1,478 km of airborne data were acquired during 18 hours of flight time over a nine-day survey period (Hefford, 2001). Instruments aboard the aircraft acquired TDEM and magnetic field data simultaneously.

The TDEM method (Kaufman and Keller, 1983; Spies and Frischknecht, 1991) used in the airborne survey measures the decay of a transient, secondary magnetic field produced by the termination of an alternating primary electric current in the transmitter loop (fig. 5). The secondary field, generated by current induced to flow in the ground, is measured by the receiving coil

Table 2. Survey and flight parameters for the Sterling County airborne survey acquired by Fugro Airborne Surveys.

Acquisition date	August 26 to September 3, 2001
Aircraft	DeHavilland DHCC-7EM (Dash 7)
Principal line spacing	100 m
Tie line spacing	4,000 m
Principal line, length and direction	17.8 km, 0 and 180 degrees
Tie line, length and direction	9.1 km, 90 and 270 degrees
Aircraft and transmitter height	120 m
Location	Differential GPS
Flight speed	70 m/s (420 km/hr)
Distance flown	1,478 km
Area surveyed	162 km ²

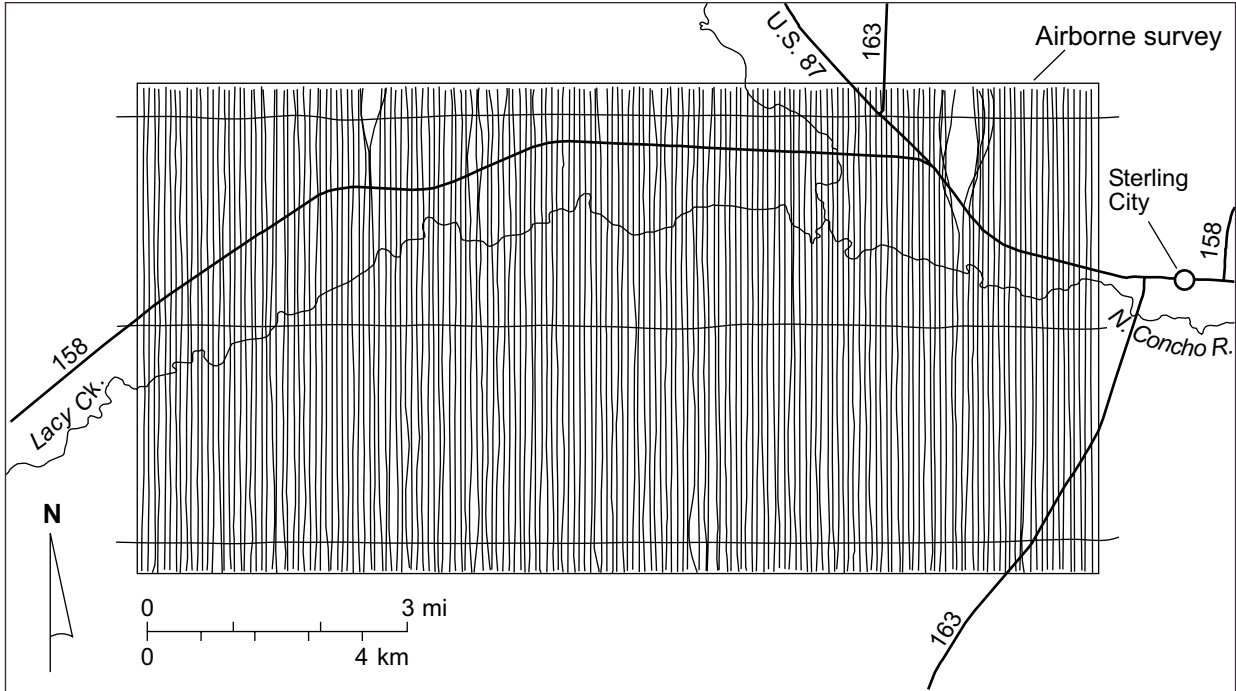
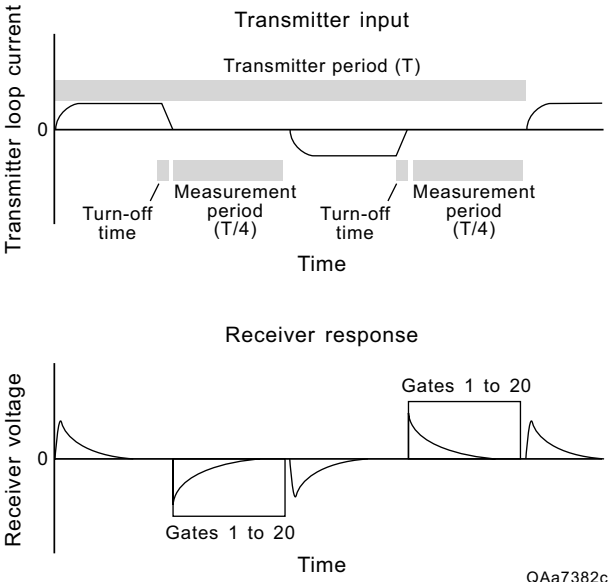


Figure 4. Flight lines flown by Fugro Airborne Surveys in August and September 2001. Open areas are tower sites.



QAa7382c

Figure 5. Time-domain EM transmitter input (upper graphic) and receiver response (lower graphic). Adapted from Geonics Limited (1992).

following transmitter current shutoff. Secondary field, or transient, strength at an early time gives information on conductivity in the shallow subsurface; transient strength at later times is influenced by conductivity at depth.

A DeHavilland Dash 7 aircraft (figs. 6 and 7) flying at a height of 120 m carried the MEGATEM II TDEM transmitter attached to the aircraft and towed a triaxial EM receiver about 131 m behind the transmitter at a height of 64 m above the ground (tables 2 and 3). The primary EM field was generated by a four-turn wire loop carrying a 1,331-ampere current at 30 Hz, resulting in a dipole moment of more than 2.1×10^6 A-m² (table 3). Each transmitter current pulse lasted 3.9 milliseconds (ms). Transients were recorded during the 11.6-ms window following termination of the transmitter input pulse. EM diffusion depth, the depth below which currents will not have diffused during the measurement period, is commonly used as a proxy for exploration depth. It is calculated using the equation

$$d = k (t r)^{0.5}$$

where d = diffusion depth (in m), $k = 503.3$ (m/ohm-s)^{0.5}, t = latest time measured, and r = resistivity (in ohm-m) (Parasnis, 1986).

Table 3. Acquisition parameters for the Sterling County airborne TDEM survey.

System	MEGATEM II
Transmitter loop area	406 m ²
Transmitter loop turns	4
Transmitter loop current	1331 A
Transmitter dipole moment	2,161,000 A-m ²
Transmitter frequency	30 Hz
Transmitter on time	3.85 ms
Receiver type	Towed 3 axis
Receiver height	64 m
Receiver trailing distance	131 m
Number of recording windows	20
Recording time (from end of pulse)	-3.6 to 11.6 ms
Sample rate	4 Hz
Sample interval	~18 m



Figure 6. The DeHavilland Dash-7 used to acquire airborne geophysical data in Sterling County.

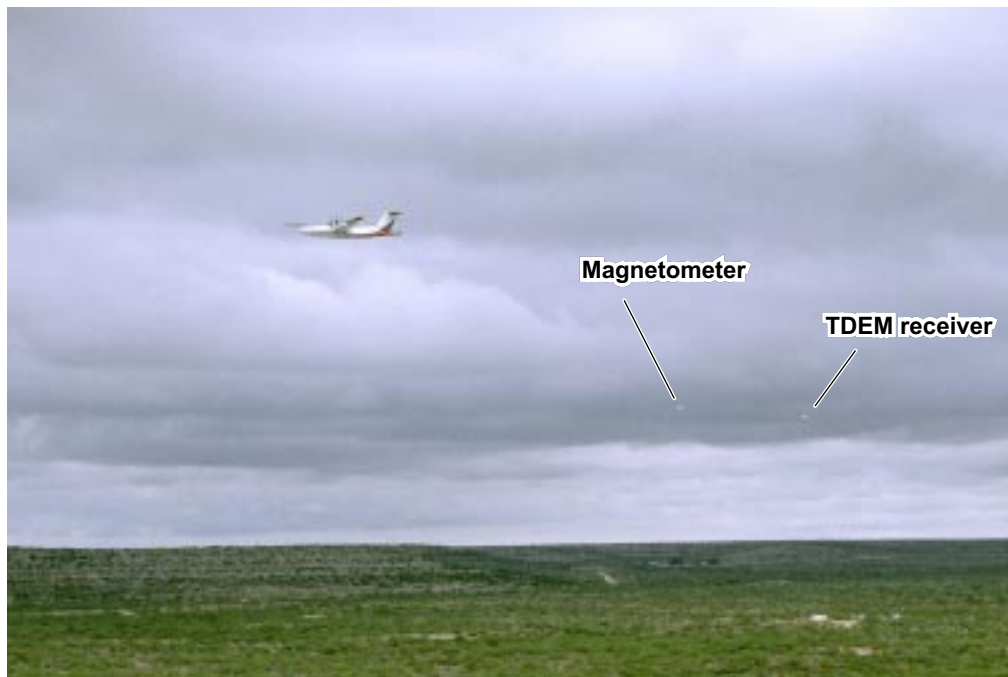


Figure 7. Survey aircraft acquiring TDEM and magnetic field data over the Parochial Bade field, August 2001.

Assuming an average ground resistivity of 20 ohm-m and a latest measurement time of 11.6 ms, exploration depth for the study area is about 240 m. Measurement locations were determined from differential global-positioning-system (GPS) data by using a base station at the San Angelo airport and a roving receiver on the aircraft. At the 30-Hz transmitter frequency (60-Hz sample frequency) and an airspeed of about 70 m/s, transients were acquired at an along-line spacing of about 1 m. Adjacent transients were stacked to reduce noise and recorded at 4 Hz, resulting in the final sample spacing of about 18 m. Fugro processed the data.

Along with the transients measured in the x (parallel to the flight path), y (horizontal and perpendicular to the flight path), and z (vertical) axes by the towed receiver coils, Fugro performed conductivity-depth transforms to produce relatively smooth conductivity models depicting a conductivity value at 10-m-depth intervals. These transforms were performed for every stacked transient.

We produced horizontal images of subsurface conductivity for each survey area by (1) extracting modeled conductivity values at 10-m-depth intervals; (2) gridding the values within the image processing software ERMapper using a cell size of 25 m; (3) rescaling the color bar to cover 99 percent of the data range (cutting off 0.5 percent of the values at the low and high “tails” of the data spectra), and (4) exporting the georeferenced images using the Universal Transverse Mercator (UTM) zone 14 north projection and the 1983 North American Datum.

Digital images were imported into a GIS database. Coverages used to analyze the relationship between the geophysical data and geological and hydrological characteristics of the region included water-well locations and depths, water-quality analyses, roads (and associated power lines), streams, oil and gas wells, and pipelines.

The aircraft also towed a cesium magnetometer at a height of 73 m above the ground (table 4 and fig. 7) to measure changes in the magnetic field strength caused by natural effects and local features such as oil and gas wells that contain significant amounts of iron. Magnetometer data were acquired at 10 Hz, yielding a 7-m sample spacing for magnetic field data.

Table 4. Acquisition parameters for the Sterling County airborne magnetometer survey.

Magnetometer	Towed cesium vapor
Magnetometer height	73 m
Sample rate	10 Hz
Sample interval	~7 m
Sensitivity	0.01 nT

GROUNDWATER DEPTH

To ensure that the exploration depth of the airborne and ground-based geophysical instruments is sufficient to reveal information about groundwater salinization, we examined water depths reported from 75 wells within the survey area (fig. 8). These data indicate that depth to water ranges from about 4 to 94 m, averaging 26 m (fig. 9). Surface elevation also varies significantly across the study area, ranging from below 700 m in the Lacy Creek valley to more than 800 m on the upland. There is a strong correlation between surface elevation and water depth: as elevation increases, depth to water also increases. In general, the elevation of the water table mimics the surface elevation (fig. 10); groundwater beneath the uplands has higher water-table elevations than does groundwater in the valleys. Well depths, reported for 69 wells in the survey area, range from about 6 to 120 m. Calculated airborne geophysical exploration depths greater than 200 m exceed the depths of the deepest water wells reported.

GROUNDWATER QUALITY

Most of the water wells in the study area produce water from an alluvial aquifer in near-surface, unconsolidated sediments or from the Antlers Sand, a lower Cretaceous formation composed of sandstone, quartzite, conglomerate, and thin clay layers (Renfro, 1993). Of the 75 study-area wells in the TWDB data base, 40 are classified as producing from the Antlers, 29 from alluvium, and 4 from combined alluvial and bedrock aquifers.

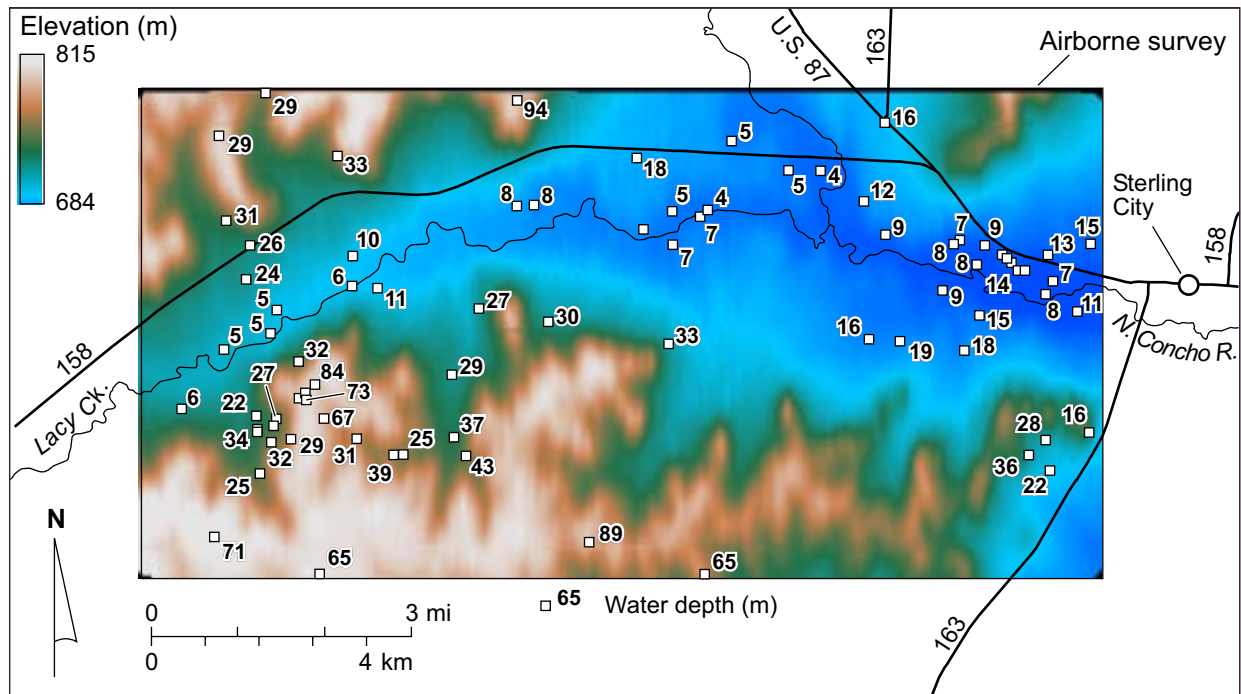


Figure 8. Location and water depths of water wells in the airborne survey area. Locations plotted on a map of land-surface elevation determined during the airborne survey. Water data from the Texas Water Development Board (TWDB).

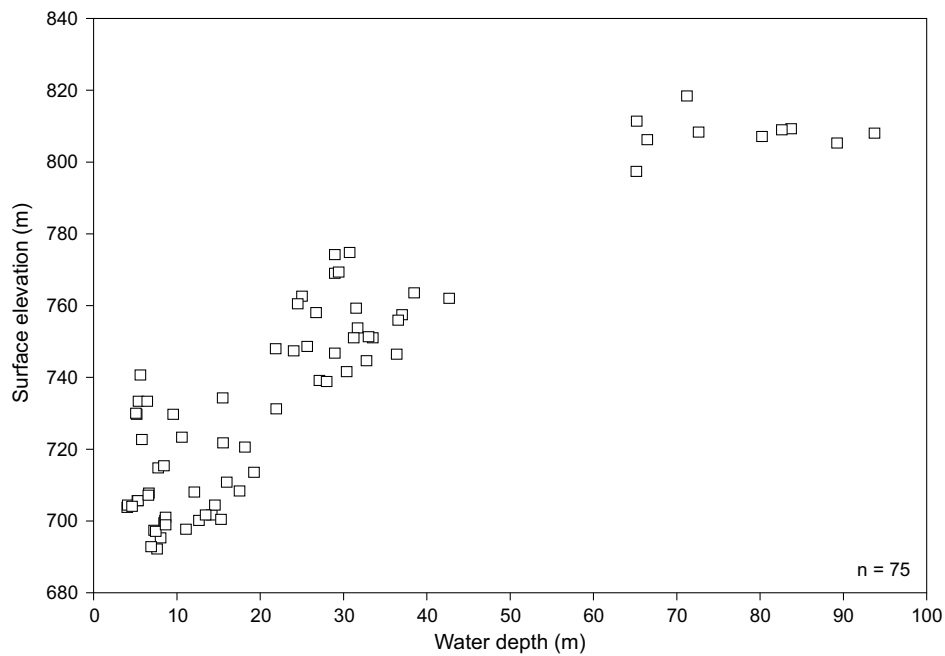


Figure 9. Relationship between water depth and surface elevation for 75 water wells within the airborne survey area. Data from the TWDB.

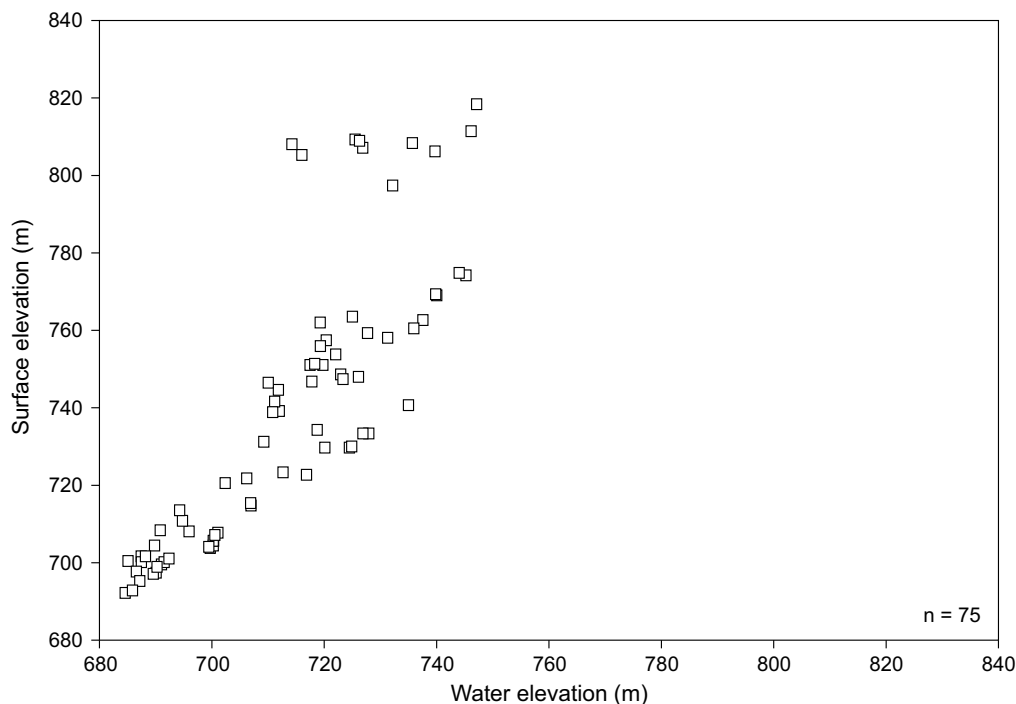


Figure 10. Relationship between land-surface elevation and water elevation in 75 water wells within the airborne survey area. Data from the TWDB.

Water produced from survey-area wells is dominantly fresh to slightly saline (fig. 11), following the total-dissolved-solids (TDS)-based classification (table 5) of Robinove and others (1958). Reported TDS concentrations range from fresh water at 238 mg/L to very saline water at 26,035 mg/L, but only four of the 53 analyses have TDS values higher than 3,000 mg/L and are classified as moderately to very saline. Chloride and bicarbonate are the most abundant anions in the reported analyses. Chloride has the highest average concentration in the 53 reported analyses at 878 mg/L (fig. 12) and is the dominant anion in the 12 samples with TDS values higher than 1,600 mg/L. At least nine of these high TDS samples are from wells and test holes that have been reported to be impacted by oilfield activities (Renfro, 1993). At the lower TDS values typical of most water samples in this area, bicarbonate is the dominant anion at average concentrations of 336 mg/L.

The dominant cations by concentration (fig. 13) are sodium (average concentration 515 mg/L) and calcium (139 mg/L). Extremely high sodium concentrations in a few samples

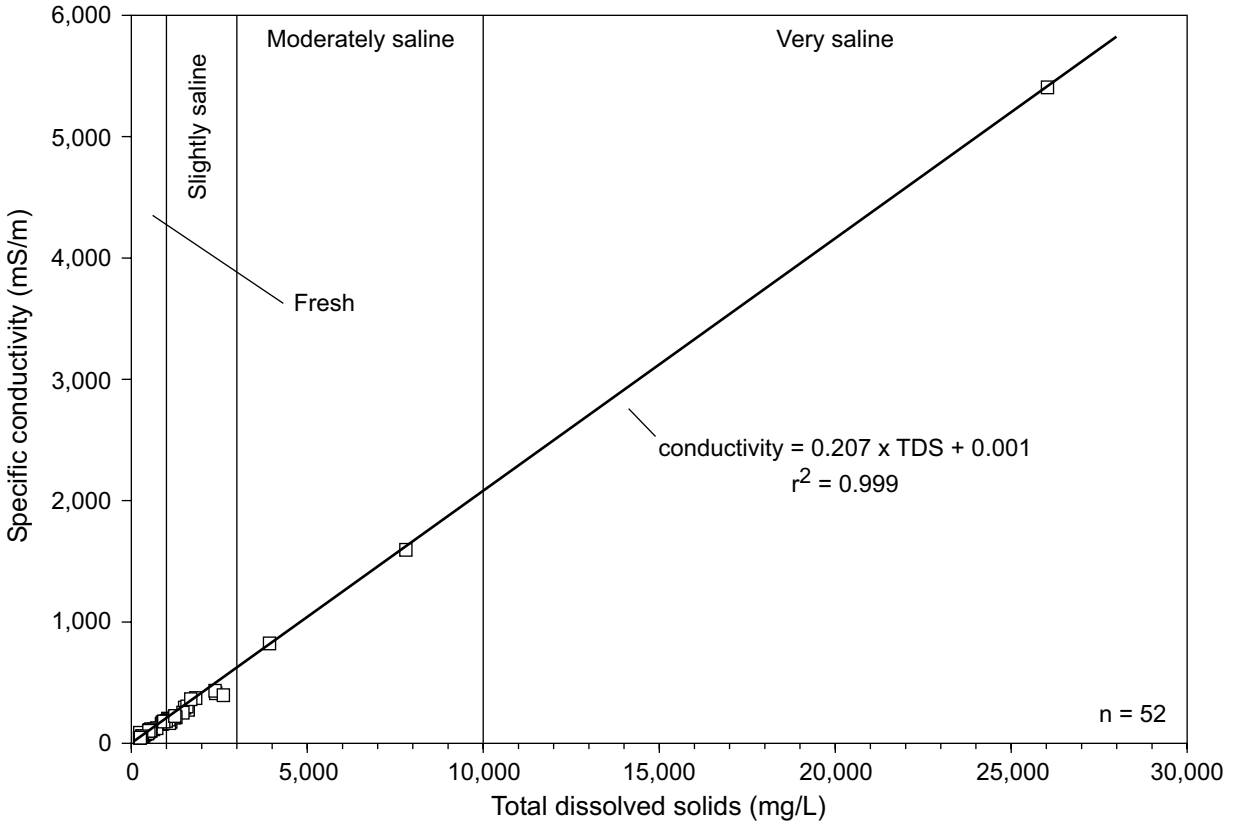


Figure 11. Relationship between total dissolved solids (TDS) concentration and specific conductivity of samples from 52 water wells within the airborne survey area. Data from the TWDB. Water salinity classification from Robinove and others (1958).

Table 5. Salinity classifications based on TDS concentration. The Robinove and others (1958) classification is used in this report because it has more subdivisions within the 0 to 5,000 mg/L TDS range that encompasses most Sterling County ground-water samples.

From Robinove and others (1958)

Classification	TDS range (mg/L)
Fresh	0 - 1,000
Slightly saline	1,000 - 3,000
Moderately saline	3,000 - 10,000
Very saline	10,000 - 35,000
Briny	35,000

From Freeze and Cherry (1979)

Classification	TDS range (mg/L)
Fresh	0 - 1,000
Brackish	1,000 - 10,000
Saline	10,000 - 100,000
Brine	100,000

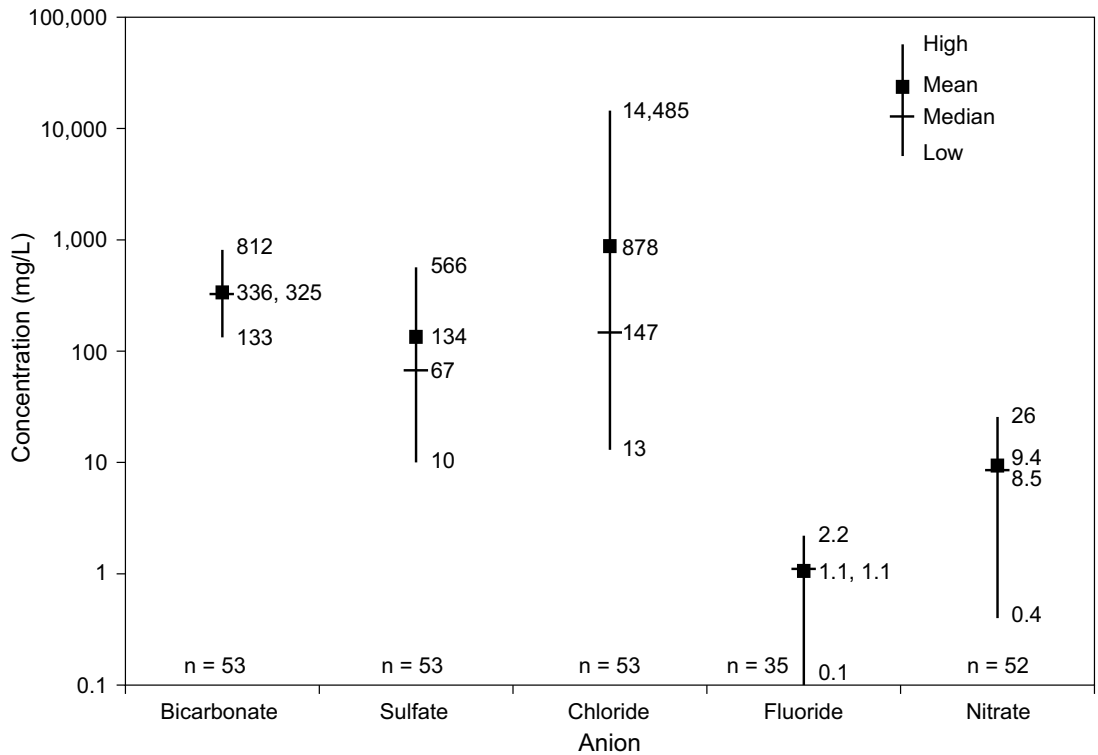


Figure 12. High, mean, median, and low concentrations of common anions in samples from water wells within the airborne survey area. Data from the TWDB.

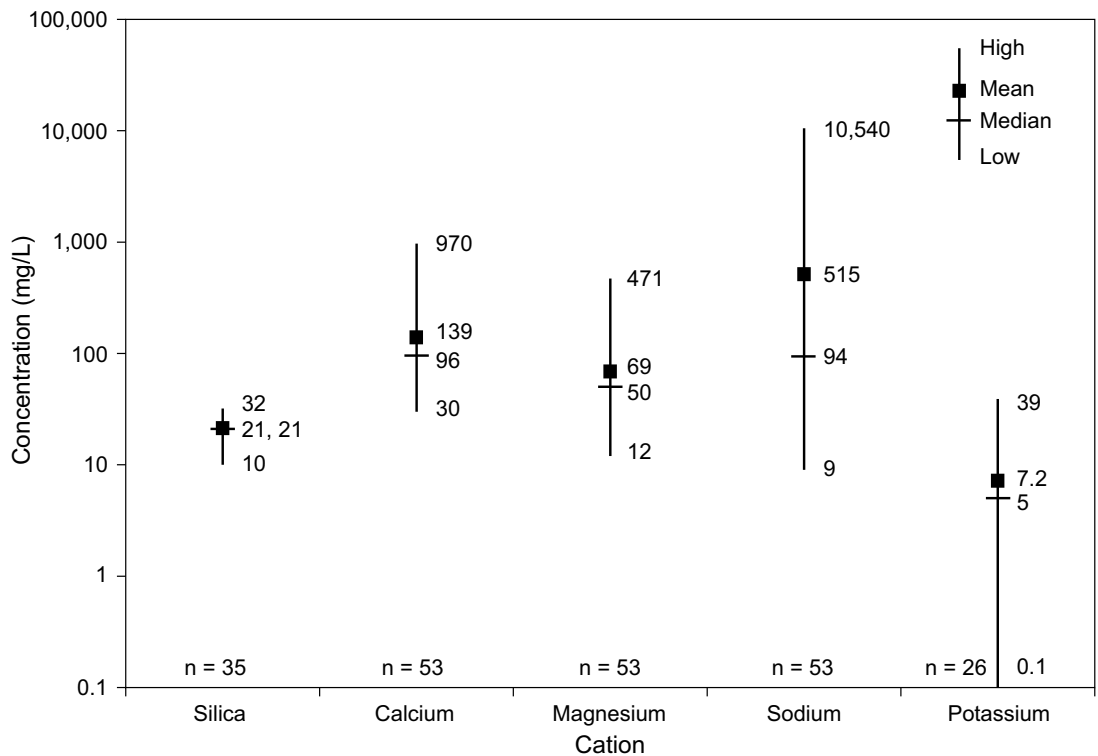


Figure 13. High, mean, median, and low concentrations of common cations in samples from water wells within the airborne survey area. Data from the TWDB.

raise the average sodium concentrations well above the median concentration of only 94 mg/L. In all moderately to very saline samples, sodium is the most abundant cation. Calcium is the most abundant cation in 29 of the 33 fresh samples.

One of the keys to the potential success of airborne EM is the relationship between TDS concentration and the electrical conductivity of water. The 52 water samples for which both specific conductance and TDS were measured show a very good relationship between TDS and electrical conductivity. As TDS increases, the measured conductivity of the water sample increases linearly at a rate of 0.2 mS/m per 1 mg/L increase in TDS concentration (fig. 11). Groundwater conductivity in the survey area is relatively low because TDS concentrations are relatively low. Only three water samples have conductivities that exceed 500 mS/m, suggesting that, in most parts of the study area, rock properties will have a strong relative influence on measured conductivities of the ground. Highly conductive ground (more than 200 mS/m) is expected only in areas where groundwater is moderately to very saline. Elsewhere, low TDS concentrations combined with relatively nonconductive soil, sediment, and rock should yield apparent ground conductivities of 200 mS/m or less.

MAGNETIC FIELD DATA

The magnetic field strength measured by the airborne magnetometer ranged from 49,464 to 49,660 nanoteslas (nT) over the survey area. To enhance local magnetic anomalies that are caused by significant iron-bearing materials such as wells, pipelines, and some structures, the regional gradient of gradually increasing magnetic-field strength to the northeast can be removed. The resulting residual magnetic intensity map (fig. 14) shows a few linear anomalies corresponding to major pipelines and hundreds of small anomalies that are tens of meters across and a few to several tens of nT in magnitude. Most of these anomalies correspond to oil and gas well locations that have been obtained from the RRC files, or, if a well location is erroneous, to visual evidence of a well location from high-resolution aerial photographs taken in 1996 (fig. 3).

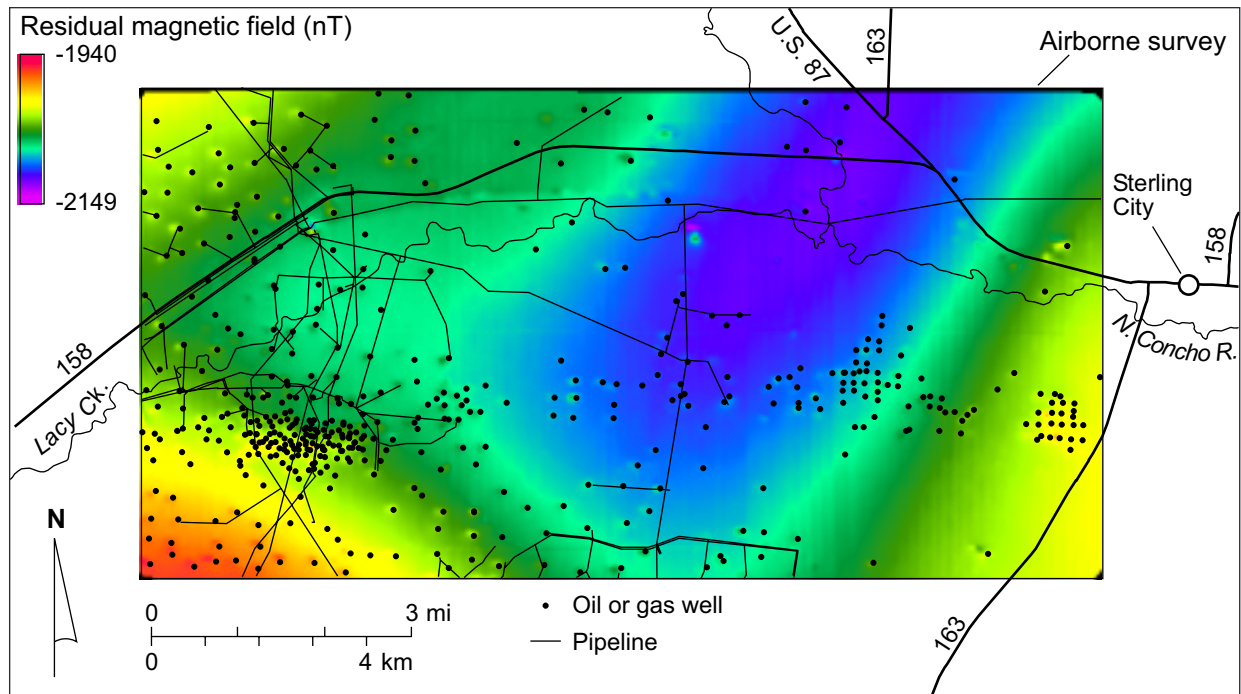


Figure 14. Residual magnetic field intensity measured during the airborne survey. Also shown are oil and gas well locations and pipeline locations from the RRC.

A few known wells, particularly those that are midway between adjacent flight lines, produce a magnetic field anomaly that was not detected by the airborne magnetometer. The airborne magnetometer distinguishes individual wells best where they are spaced farther than about 100-m apart. At closer well spacings, such as in the Parochial Bade field in the southwestern part of the survey area, the signatures of several adjacent wells can combine to form a single anomaly. Individual, densely clustered wells cannot be distinguished in these areas without tighter flight spacings or ground-based measurements.

AIRBORNE EM DATA

The principal data recorded by the airborne instruments are the decays of secondary fields generated in the ground as the transmitter loop flies overhead. These signals are recorded in the vertical and two horizontal directions and are proportional to the conductivity of the ground.

Highly conductive bodies such as metallic structures and strong fields generated by electrical power lines can modify or disrupt the secondary signal and can render conductivity models generated from the EM data invalid. As a safeguard against misinterpreting EM data, Fugro recorded the strength of power-line noise while the survey progressed. Noise levels were low across most of the survey area (fig. 15), averaging a few millivolts (mV), but were as high as 318 mV near major power lines. The high noise areas include a corridor through the middle part of the Parochial Bade field, but most oil and gas wells are in low-noise areas.

Apparent Conductance

General conductivity trends are evident in the apparent conductance map (fig. 16). Apparent conductance represents the single value at a measurement point that best fits the observed transient decay at that point, without regard for vertical distribution of conductive material. As such, maps of apparent conductance represent a first-order screening for significant differences in the electrical properties of the ground. The majority (99 percent) of conductance values are between a low of 253 mS and a high of 3,691 mS and are highly correlated to surface elevation (compare figs. 8 and 16). At higher elevations, where poorly conductive Segovia and Fort Terrett Formation limestones cap the plateaus (Eifler and Barnes, 1974), apparent conductance values are relatively low. At lower elevations, where Edwards Group limestones are thin or absent and more conductive alluvium and underlying Cretaceous Antlers Sand and older strata are present, conductance values are relatively high. Highest conductances are located along Lacy Creek in the western part of the survey area and within parts of the Parochial Bade field. The conductances within the Parochial Bade field are higher than those in other valleys at similar elevations and are also associated with the locations of shallow water wells with high TDS values.

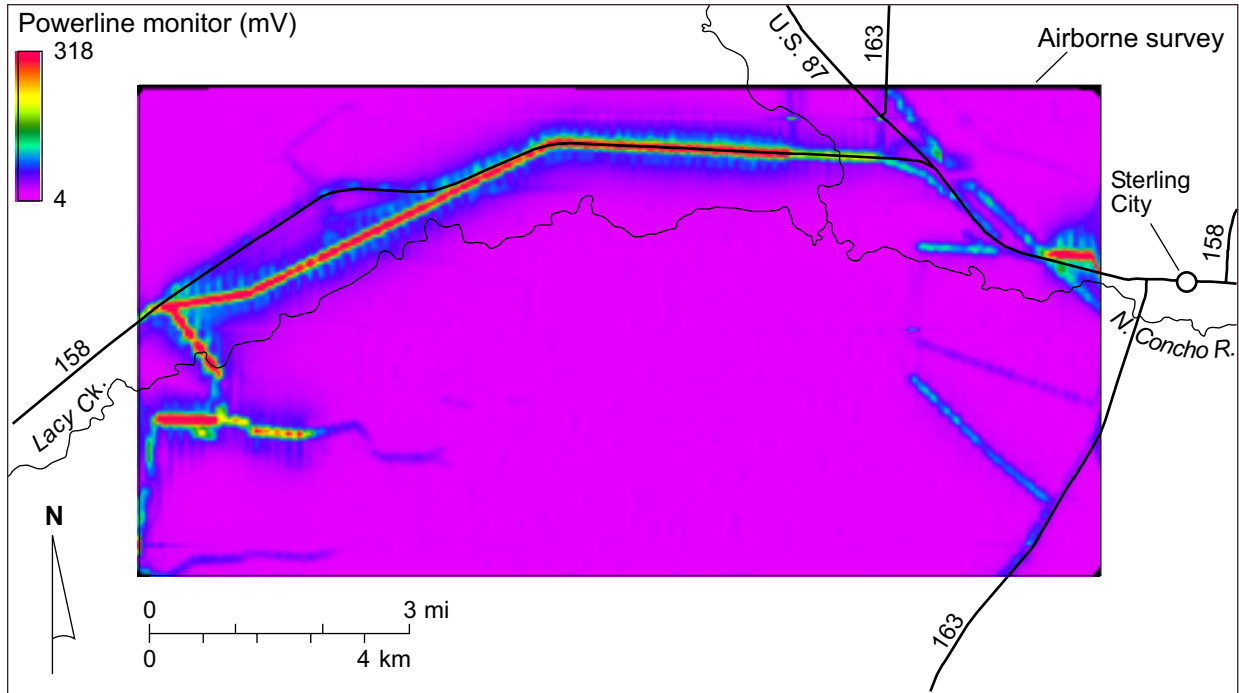


Figure 15. Powerline noise intensity measured during the airborne survey.

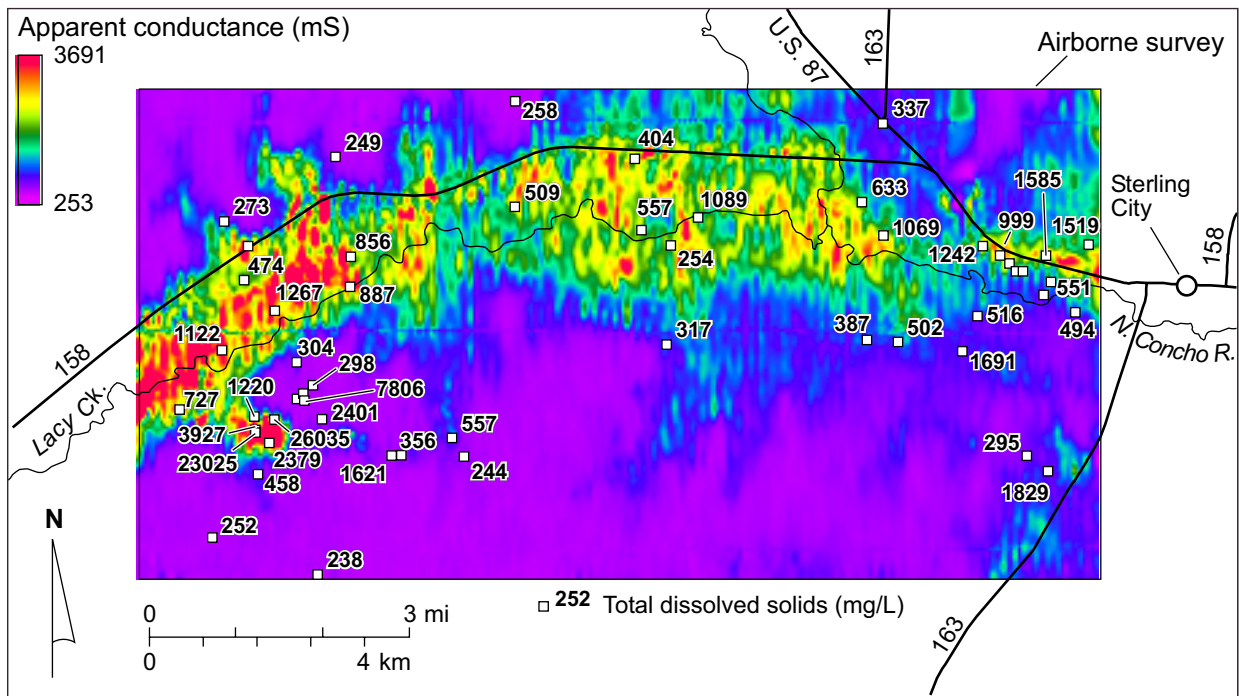


Figure 16. Apparent conductance calculated from TDEM data collected during the airborne survey. Also shown are water-well locations with TDS concentrations. Water data from the TWDB.

Conductivity-Depth Slices

Fugro processed raw airborne EM data to transform the recorded EM field decays into models of conductivity changes with depth at each measurement location. Conductivity values at common depths across the survey area can be combined to produce images of conductivity at selected depths. Most of the 108,620 conductivity models were valid to depths of at least 300 m. Because water-well depths in the area are less than 100 m, we focused on conductivity slices at 10-m intervals between 10 and 200 m below the ground surface (figs. A1 to A20). Depth slices facilitate comparison with well and water depths, but make it more difficult to interpret conductivity patterns over an area that has significant topographic relief of more than 130 m.

In general, conductivity values within the upper 300 m in the survey area are relatively low. The highest apparent conductivity values are observed on depth slices from the upper few tens of meters. For example, 99.5 percent of the calculated conductivity values are below 179 mS/m at 30-m depth. At 60-m depth, 99.5 percent of the values are below 174 mS/m. At 90 m, the upper conductivity limit is 162 mS/m, and at 120 m, the upper limit is 134 mS/m. The upper limit continues to drop for conductivity slices from deeper depths.

The conductivity slice at 10-m depth (fig. A1) reveals two areas of relatively high conductivity. The first is an area about 1 km east–west by 0.8 km north–south located in the western part of the Parochial Bade field. A second area of elevated conductivity is just downstream from the confluence of Lacy Creek and the North Concho River. Water samples of various vintages from nine wells that have depths at or deeper than 10 m and water levels at or shallower than 10 m (table 6) have fresh to slightly saline TDS values ranging from 254 to 1,242 mg/L (fig. A1). The two highest values are located within relatively conductive zones on the east side of the survey area.

At the 20-m depth, apparent conductivities remain elevated within the Parochial Bade field and near the Lacy–North Concho confluence (fig. A2). Small areas of elevated conductivity are visible elsewhere. Water-quality data interpreted to be from this depth range include fresh to

Table 6. Wells used to compare water quality and apparent conductivity measured during the airborne geophysical survey. Well data from the TWDB.

Well	Lat. (°)	Long. (°)	Elev. (m)	Well depth (m)	Water level (m)	Sample year	Sample depth (m)	TDS (mg/L)	Cond. depth (m)	App. cond. (mS/m)
4415201	31.8339	-101.1683	747	37	24	1961		474	30	52
4415205	31.8436	-101.1725	751	42	31	1968		273	40	22
4415206	31.8394	-101.1678	749	40	26	1985		303	30	13
4415302	31.8547	-101.1508	751	43	33	1968		249	40	68
4415303	31.8381	-101.1475	730	17	10	1969		856	10	23
4415506	31.8119	-101.1806	741	42	6	1992	18	727	20	84
4415507	31.8219	-101.1725	733		6	1992		1122		
4415603	31.8050	-101.1369	763	35	25	1992		356	30	46
4415604	31.8081	-101.1269	757	54	37	1968		557	50	33
4415605	31.8139	-101.1561	808	94	73	1992		7806	90	134
4415608	31.8067	-101.1628	759	53	32	1998		2379	50	122
4415609	31.8086	-101.1656	751	63	34	1992		3927	60	96
4415610	31.8083	-101.1656	751			1989		23025		
4415611	31.8108	-101.1525	806	119	66	1992	76	2401	80	73
4415612	31.8142	-101.1575	807	110	80	1992	77	2620	80	85
4415613	31.8203	-101.1578	754	62	32	1992	49	304	50	68
4415614	31.8150	-101.1564	809	116	83	1992	101	1470	100	126
4415615	31.8164	-101.1544	809	113	84	1992	92	298	90	83
4415616	31.8106	-101.1619	758	65	27	1992	28	26035	30	28
4415618	31.8289	-101.1622	730	32	5	1992	18	1267	20	25
4415619	31.8331	-101.1475	723	23	6	1992	15	887	10	31
4415620	31.8111	-101.1658	748	30	22	1992	27	1220	30	100
4415621	31.8014	-101.1650	760	31	25	1992	29	458	30	63
4415623	31.8050	-101.1386	764	60	38	1992	52	1621	50	44
4415801	31.7906	-101.1736	818	105	71	1968		252	100	62
4415901	31.7847	-101.1528	811		65	1992		238		
4416101	31.8469	-101.1156	715	11	8	1969		509	10	17
4416103	31.8556	-101.0922	721	32	18	1985		404	30	52
4416105	31.8411	-101.0847	708	22	7	1969		254	10	47
4416106	31.8433	-101.0906	712			1969		557		
4416108	31.8647	-101.1158	808	110	94	2001		258	100	103
4416205	31.8458	-101.0794	707		7	1969		1089		
4416206	31.8489	-101.0475	708	14	12	1969		633	10	50
4416207	31.8433	-101.0431	700	10	9	1967		1069	10	57
4416208	31.8622	-101.0436	722	91	16	1985	30	337	30	65
4416301	31.8339	-101.0114	692	85	8	1968		551	30	34
4416303	31.8403	-101.0200	701	27	9	1982	9	999	10	97
4416304	31.8378	-101.0156	695	21		1982		914	20	75
4416306	31.8392	-101.0183	702	36	14	1969		1040	20	53
4416310	31.8425	-101.0028	700	25	15	1982	17	1519	20	62
4416312	31.8406	-101.0111	700		13	1982	12	1585	20	96
4416313	31.8361	-101.0100	693	58	7	1982	7	925	10	54
4416314	31.8378	-101.0169	696			1982		884		
4416315	31.8419	-101.0236	699	33	9	1982	9	1242	10	185
4416403	31.8050	-101.1244	762	49	43	1968		244	50	45
4416405	31.8244	-101.0853	745	37	33	1969		317	30	70
4416503	31.8258	-101.0458	711	23	16	1969		387	20	81
4416603	31.8311	-101.0053	698	32	11	1969		494	20	131
4416604	31.8256	-101.0400	714	26	19	1969		502	20	15
4416605	31.8303	-101.0244	704	23	15	1969		516	20	69
4416606	31.8242	-101.0272	708	27	18	1969		1691	20	29
4416608	31.8069	-101.0142	746	43	36	1969		295	40	23
4416609	31.8044	-101.0100	731	61	22	1969		1829	30	72

slightly saline TDS values from 11 wells, most of which are on the eastern side of the study area (fig. A2). Low TDS values (below 1,000 mg/L) tend to be from low-conductivity areas, whereas three of the highest TDS values (above 1,000 mg/L) are from an area of elevated conductivity northwest of Sterling City.

Conductivities at 30-m depth remain elevated northwest of Sterling City and in the Parochial Bade field area (fig. A3). The highest TDS value reported for the area, 26,035 mg/L in Test Hole #6 in the Parochial Bade field, is reported within this area of elevated conductivity, as is the slightly saline TDS value from another nearby well. Lower TDS values characteristic of fresh water are reported at this approximate depth elsewhere in the survey area.

At 40 m, apparent conductivity remains elevated in the Parochial Bade area and in the large area northwest of Sterling City (fig. A4). A smaller zone of elevated conductivity extends about 800 m east–west and 1,100 m north–south along the southern edge of Lacy Creek about 4 km from the western edge of the survey area. Only three TDS values are interpreted to be from this depth range; all of these samples have low TDS values (249 to 273 mg/L) and are from areas shown to have relatively low conductivity at that depth.

The four water wells that have TDS values interpreted to be from the 50-m depth range show good agreement with apparent conductivity patterns at that depth (fig. A5). High, slightly saline TDS values (1,621 and 2,379 mg/L) are located within areas of elevated conductivity in the Parochial Bade field. Lower, fresh-water TDS values of 244 to 557 mg/L are located in areas of relatively low apparent conductivity within and around the perimeter of the field. The zone of elevated conductivity along Lacy Creek is larger than it appears at the 40-m depth, but no water samples are available from wells in that area. Apparent conductivity remains high in the northeastern part of the survey area, north and east of the North Concho River.

The 60-m conductivity slice (fig. A6) continues to show elevated conductivities around the Parochial Bade field, along Lacy Creek downstream from the field, and northwest of Sterling City. One water well sample interpreted to be from this depth range has a moderately saline TDS

value of 3,927 mg/L and is located within the area of elevated conductivity at the Parochial Bade field.

Conductivity patterns in the 70- to 100-m depth range are similar to those at 60 m (figs. A7 to A10). The zone of elevated conductivity about 4 km from the western survey boundary along Lacy Creek that is evident at the 40- to 60-m depths appears to migrate southward with depth, reflecting the increase in elevation from the valley floor along the creek to the plateau. Conductivities in and near the Parochial Bade field become less anomalous with depth. Two water samples interpreted to be from the 80-m depth range show slightly saline TDS values within the zone of elevated conductivity associated with the Parochial Bade field (fig. A8). At 90 m, one fresh and one moderately saline water sample are interpreted to be from this depth range on the northern margin of the field. At 100 m, the highest apparent conductivities are depicted on the southwest and northwest corners of the survey area. Three fresh to slightly saline water analyses are interpreted to be from this depth range; the highest TDS value is reported for Test Hole #4 on the plateau above the Parochial Bade field.

By the 110-m depth, the depths of all the reported water wells in the survey area have been exceeded. Conductivity slices from deeper depths (figs. A11 to A20) mostly penetrate stratigraphic levels that are well beyond the Antlers Sand. These slices show continued elevated conductivity values in the northwest and southwest part of the survey area. Deeper than 130 m, a zone of elevated conductivity is evident in the eastern part of the survey area, southwest of Sterling City, in the approximate area of the Durham Oil Field. Elevated conductivities in this area appear to expand and migrate westward as depth increases to 200 m, the deepest level shown. No water-well data are available from this depth that would distinguish among possible causes of elevated conductivity that include a naturally conductive formation or lateral infiltration of injected water produced from the Durham field.

Conductivity Cross Section

Renfro (1993) includes cross section A–A' that depicts stratigraphic and hydrologic data from wells drilled for the RRC during an investigation of a salinized water well on the Price ranch. Another way to view the airborne EM data is to construct cross sections composed of apparent conductivity profiles at a given set of measurement locations. We used 14 conductivity profiles located as close as possible to the cross section shown in Price (1993) to construct a conductivity cross section that also includes some stratigraphic and hydrologic data (figs. 17 and 18). Each profile is constructed of the same conductivity values at 10-m depth intervals that were used to create the depth slices.

Apparent conductivity values in Edwards Group strata on the plateau above the Parochial Bade field are all well below 100 mS/m. Conductivity values increase within the Anters Sand, particularly near wells such as Test Hole #4, where an elevated TDS value of 4,878 mg/L coin-

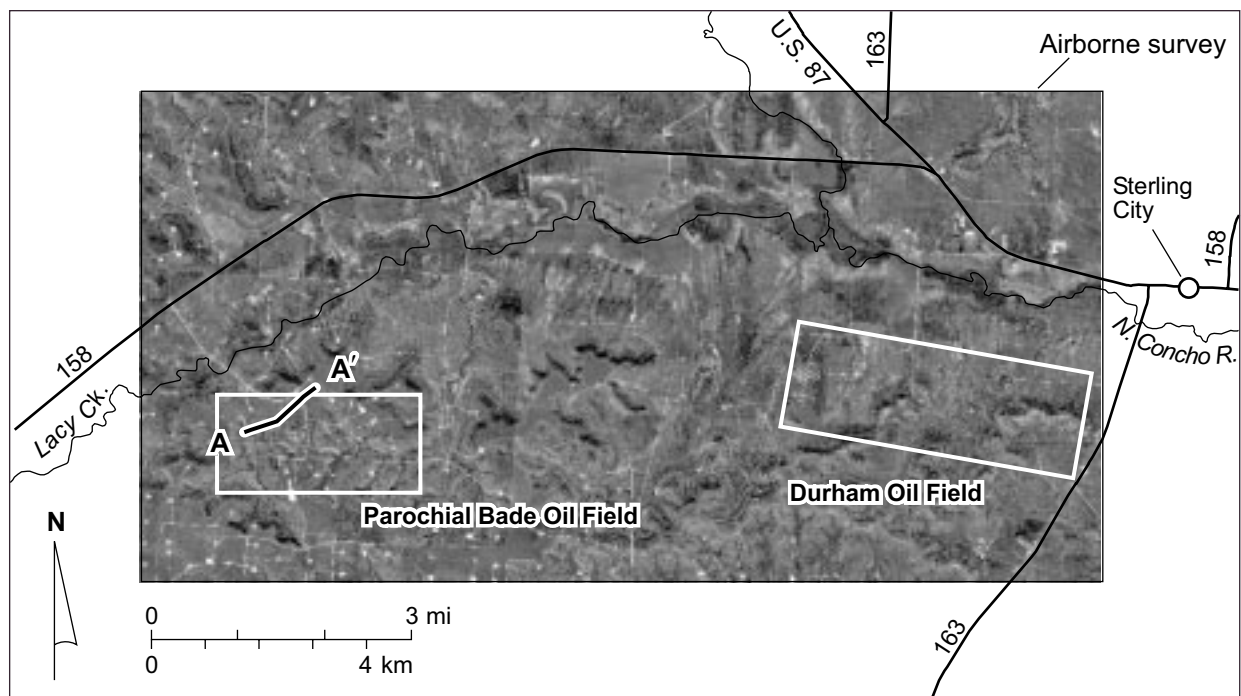


Figure 17. Locations of the Parochial Bade Oil Field, the Durham Oil Field, and cross section A–A'.

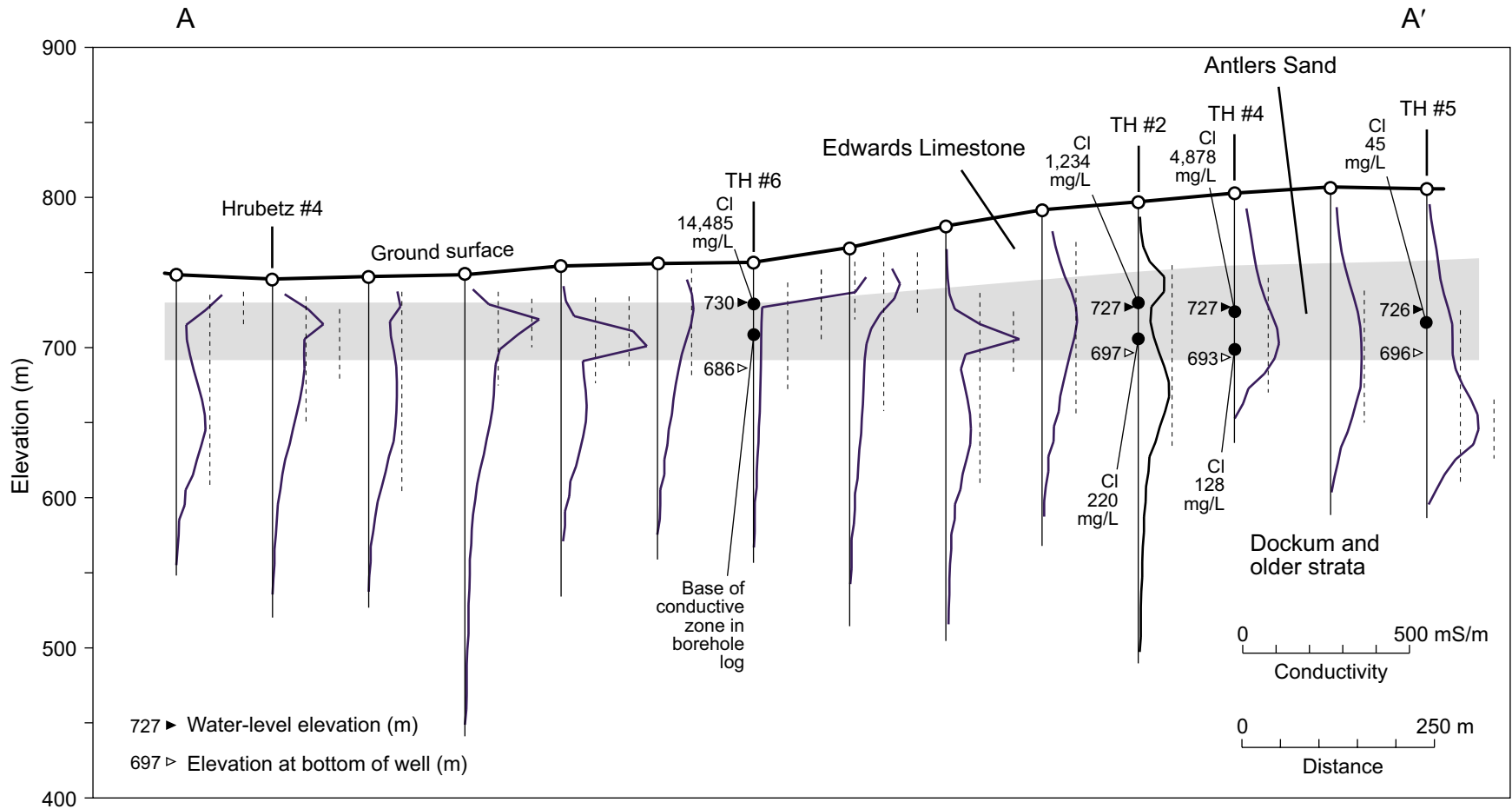


Figure 18. Cross section A–A' across the Parochial Bade field constructed from conductivity profiles extracted from the airborne geophysical data. The section corresponds to that in Renfro (1993) and includes stratigraphic and hydrologic data from that report.

cides with an apparent conductivity value higher than 100 mS/m in the nearest conductivity profile from the airborne geophysical survey. At the lower elevations in the Parochial Bade field, some profiles show highly elevated apparent conductivities above and within Antlers strata. These elevated apparent conductivities are more than 300 mS/m near Test Hole #6 and are corroborated by elevated conductivities measured using a borehole instrument during the RRC investigation (Renfro, 1993).

Quantifying the Relationship Between Conductivity and Water Salinity

Qualitative comparisons of TDS values from water samples with apparent conductivities at various depths show relatively good agreement (figs. A1 to A10). Areas with relatively high apparent conductivities at given depths tend to correlate to wells with relatively high TDS water at that depth, and areas with relatively low apparent conductivities at given depths tend to be near water wells producing relatively low TDS water at those depths. To further quantify this relationship, we attempted to extract an apparent conductivity value at the location of the well and at a depth that was shallower than the well depth but deeper than the reported water level. We found 47 water wells in the TWDB database for which there was a location, a well depth, a water level, and a TDS value (table 6). We used the reported locations of these wells to obtain an apparent conductivity at that location from the airborne geophysical data.

At this level of comparison, reported TDS values show relatively poor correlation with apparent conductivities at the specific well location and interpreted sample depth (fig. 19), which appears to contradict the reasonable geographic agreement among TDS values plotted on the conductivity maps. There are several possible explanations for the lack of a better quantitative relationship between TDS and apparent conductivity. First, most of the TDS values are for fresh to slightly saline water. At low TDS values, the conductivity of water-saturated sediments and rocks is more strongly influenced by sediment or rock type than it is at higher TDS values. Second, the airborne survey was flown in 2001, whereas chemical analyses of water samples

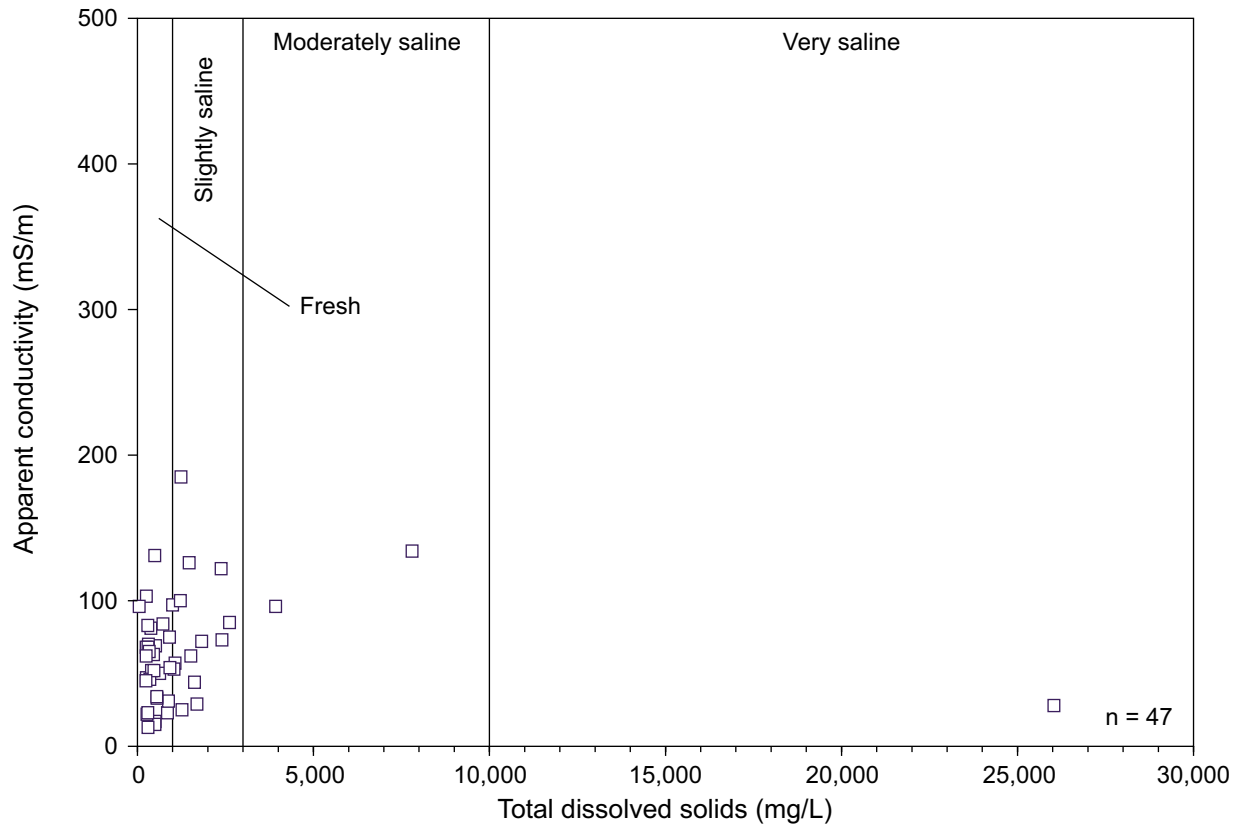


Figure 19. Relationship between TDS concentration in groundwater samples from the airborne survey area and apparent conductivities calculated from airborne data for depths below the water level and above the well depth (table 6). Water data from the TWDB.

range in age from 1961 to 2001. Third, locations of the water wells may be less accurately known than the location of the conductivity profiles. Fourth, except for a few wells, it is difficult to assess the actual stratal depth that contributed the analyzed water sample. Fifth, apparent conductivity values were determined from gridded line data rather than from the nearest actual measurement. Depending on the well distance from the original measurement, the apparent conductivity value may not represent the best estimate obtainable from the airborne geophysical data at the actual well location.

Comparison with Ground-Based EM Measurements

We acquired reconnaissance, ground-based conductivity data in January 2001 to determine background conductivity, identify potential salinization along Lacy Creek, its tributary that drains the Parochial Bade Oil Field, and near water wells where contamination has been documented, and to help select the appropriate airborne geophysical instruments. We can also use these data to verify the accuracy of airborne geophysical measurements where both types were acquired.

Line A is a short line located at the head of the draw that bisects the Parochial Bade field (fig. 3). Apparent conductivities measured along this line using the 20-m coil separation (exploration from the surface to depths of 12 to 25 m) were less than 10 mS/m (fig. 20a), the lowest measured along any ground-based transect. Edwards Group limestones crop out in this area; the low conductivities observed on the ground lines support the observation made from the apparent conductance map (fig. 16) that the plateau areas are less conductive than the valleys. The 10-m conductivity depth slice (fig. A1) also shows relatively low conductivities in this area (30 mS/m or less).

Line B is a 500-m long line along Lacy Creek just downstream from where the draw passing through the Parochial Bade field drains into the creek. At the 20-m coil separation, apparent conductivities were near 50 mS/m, increasing slightly in an upstream direction (fig. 20b). Apparent conductivities higher than those observed on the plateau are consistent with the elevated values observed in the valleys on the apparent conductance map (fig. 16) and also consistent with the presence of a shallow water table and naturally more conductive alluvial sediments. The 10- and 20-m depth slices show similar conductivity values at this location (figs. A1 and A2).

Lines C (fig. 20c) and G (fig. 20g) are coincident lines that are 1.1-km long along the draw through the Parochial Bade field. At the north, downstream end of line C, collected at the 20-m coil spacing, conductivities are about 50 mS/m and are similar to those observed near the confluence with Lacy Creek. Conductivities generally decrease southward toward the upstream

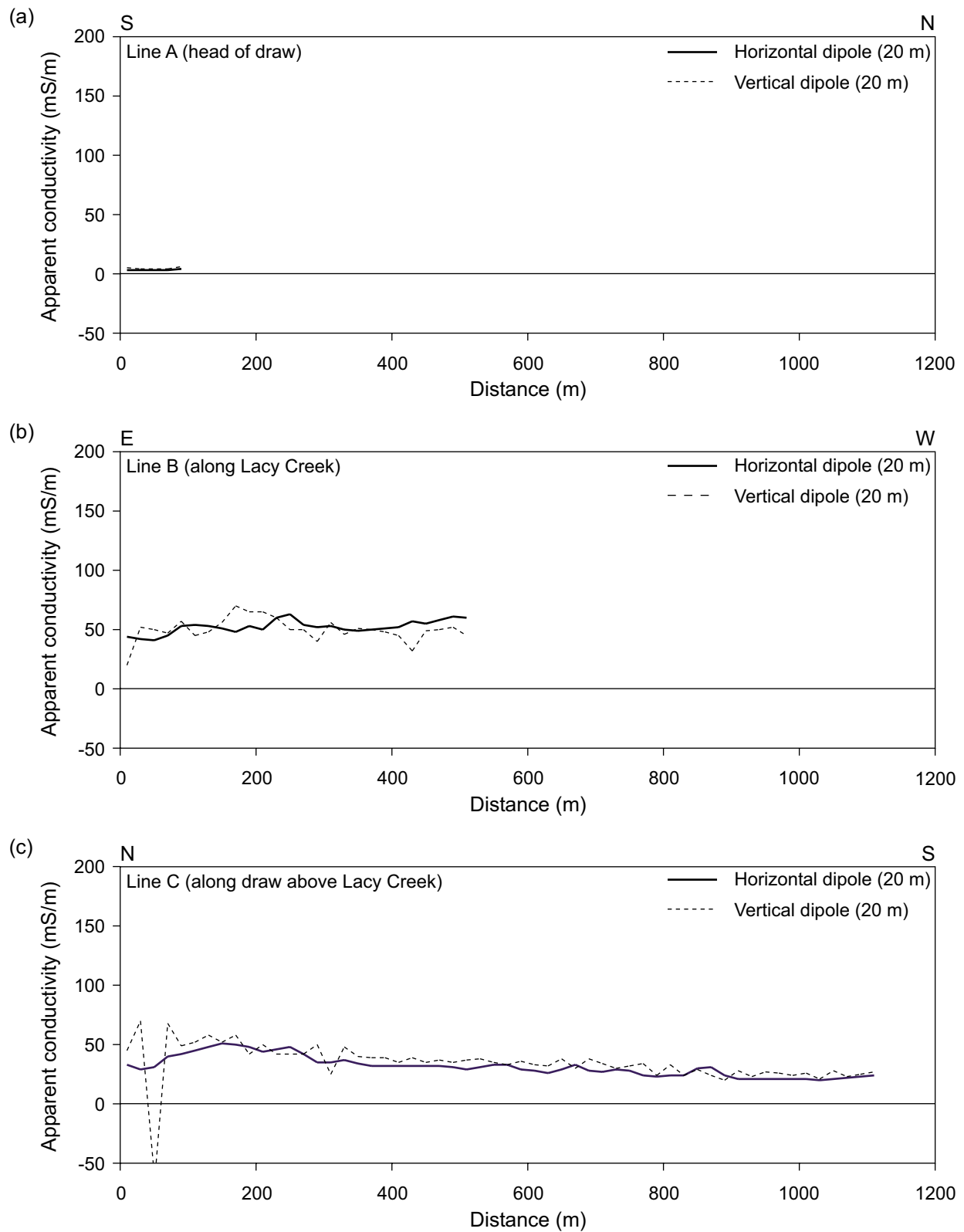


Figure 20. Apparent conductivity acquired using a ground-based conductivity meter along (a) Line A, (b) Line B, (c) Line C, (d) Line D, (e) Line E, (f) Line F, (g) Line G, (h) Line H, and (i) Line I. Locations shown on fig. 3.

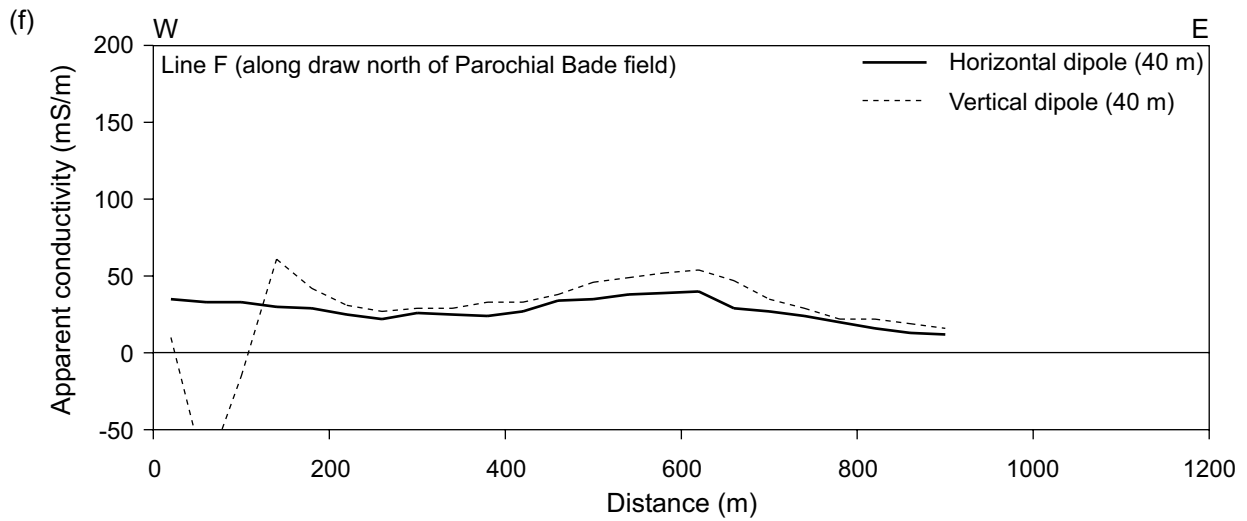
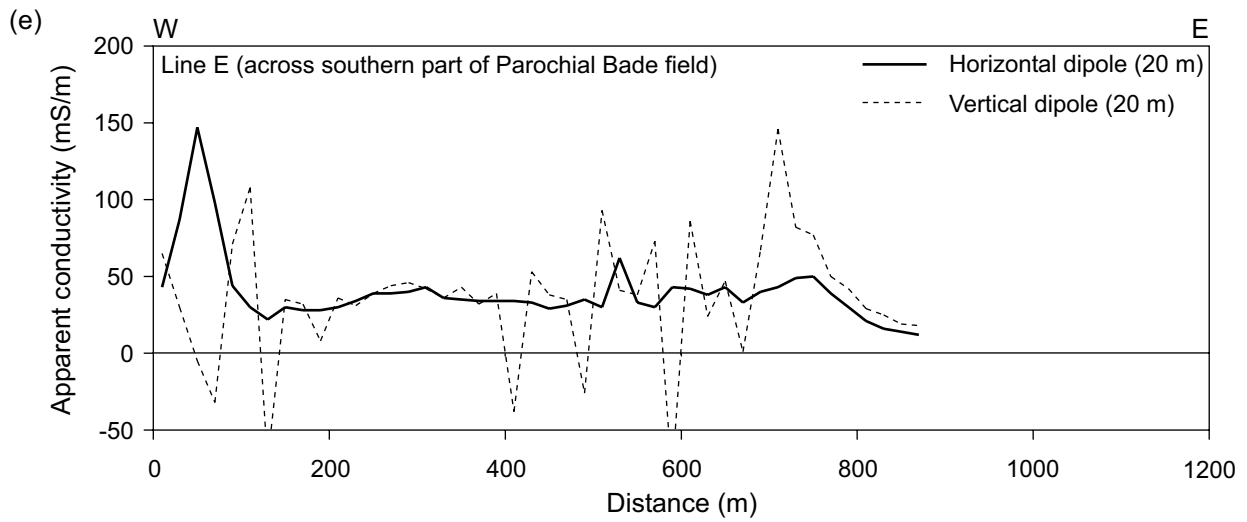
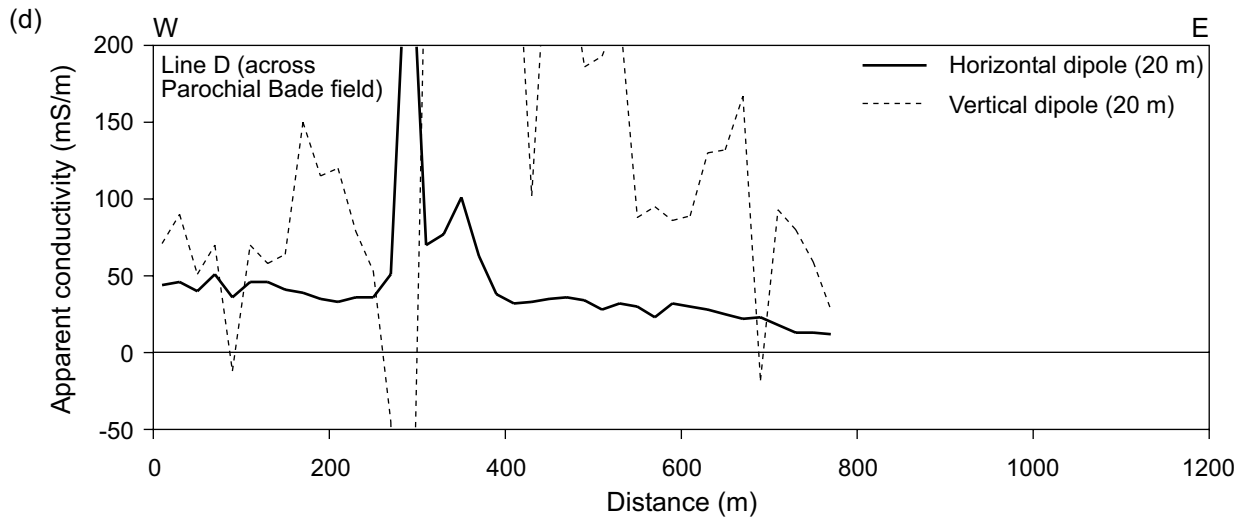


Figure 20 (continued)

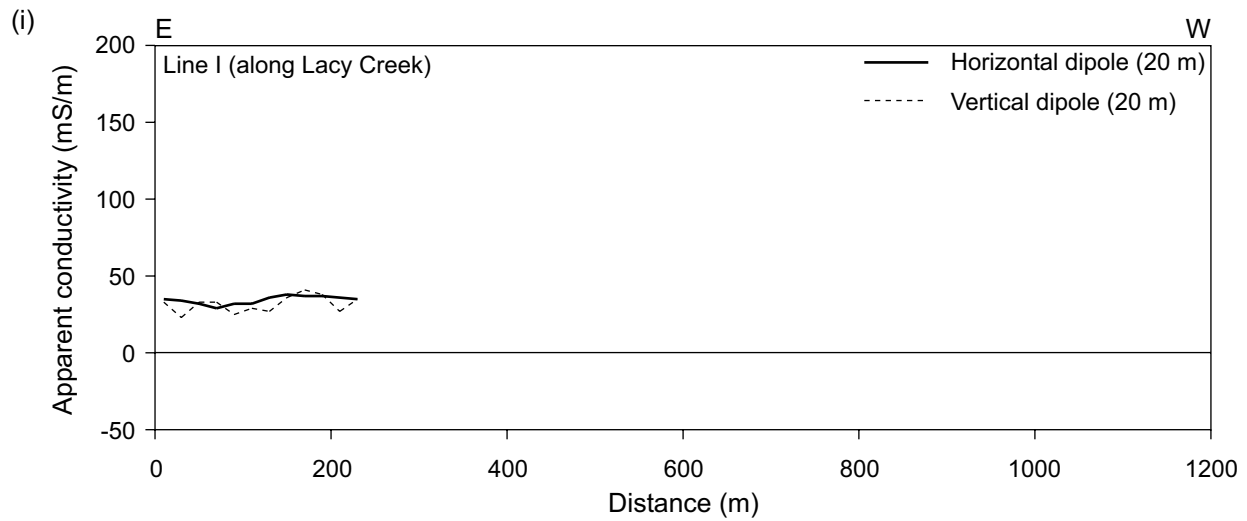
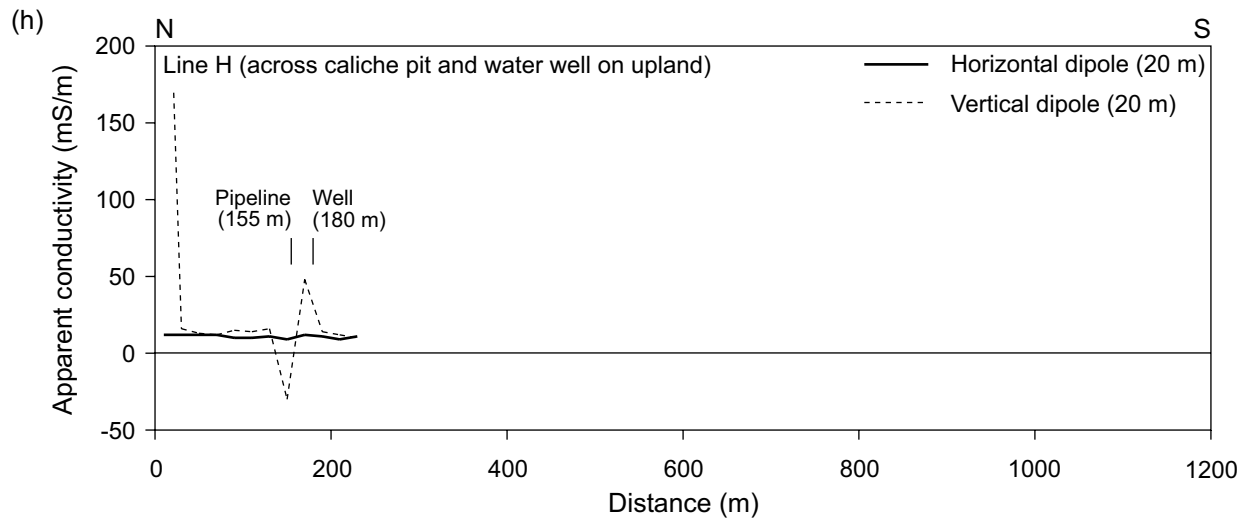
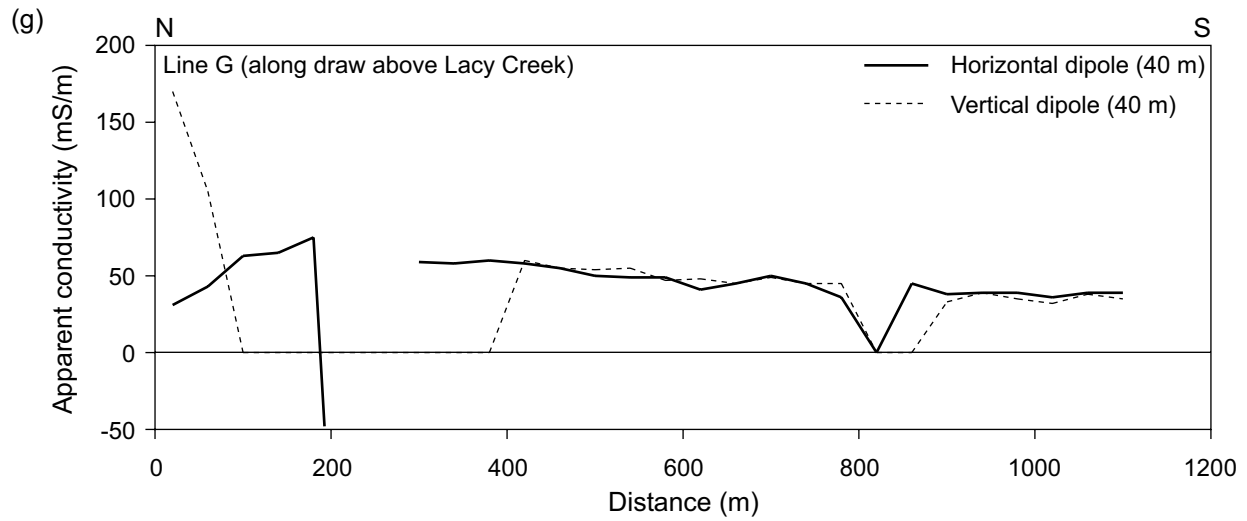


Figure 20 (continued)

end of the draw, approaching the extremely low conductivities observed at line A. The most elevated conductivities were measured between 100 and 300 m from the north end of the line, near the northwest margin of a dense concentration of Parochial Bade field wells. Similar conductivity trends at higher conductivity values are evident on line G (fig. 20g), which was acquired at the 40-m coil spacing (exploration from the surface to depths of 24 to 51 m). Conductivities exceed 50 mS/m between 100 and 300 m up the draw from the north end of the line, then gradually decrease farther south as elevation increases. The slight conductivity decrease at the north end of lines A and G suggests that the elevated values through the Parochial Bade field are caused by minor oilfield-related salinization. The conductivity decrease in the upvalley direction is most likely caused by thinning of more conductive alluvium and thickening of poorly conductive Edwards Group limestones.

Lines D, E, and F cross the Parochial Bade field in an east–west direction (fig. 3). Line D, acquired at the 20-m coil spacing, shows conductivity generally decreasing from about 50 mS/m at the draw to about 10 mS/m at the higher elevations on the east end of the line (fig. 20d). Anomalously high apparent conductivities were measured 250 to 400 m east of the draw, suggesting a local salinization source in this area. Renfro (1993) has mapped two abandoned salt-water disposal pits at this location. The 20-m conductivity depth slice from the airborne survey shows an area of high apparent conductivity (more than 100 mS/m) along this line about 220 to 450 m from the draw.

Line E, acquired at the 20-m coil separation across the southern part of the field, shows apparent conductivities below 50 mS/m along most of the line (fig. 20e). The highest values were measured a short distance east of the draw, where conductivities exceeded 100 mS/m. This area is also the mapped site of an abandoned salt-water disposal pit (Renfro, 1993). Conductivity slices at 10- and 20-m depths show locally elevated conductivities at the abandoned pit site (figs. A1 and A2).

Line F was acquired north of the field at the 40-m coil spacing (fig. 3). This line displays the expected trend of decreasing apparent conductivity from the draw eastward toward the plateau,

except for a slight elevation in both horizontal and vertical dipole measurements between 400 and 700 m east of the draw (fig. 20f). This part of the line passes about 90 m north of the location of Test Hole #6, which was drilled during the RRC investigation and encountered highly salinized water within the Antlers Sand (Renfro, 1993). The 10- and 20-m conductivity-depth slices through this area also show elevated conductivities surrounding Test Hole #6 over an area extending about 600 m east–west by about 425 m north–south (figs. A1 and A2).

Line H, acquired using a 20-m coil separation, is on the plateau northeast of the Parochial Bade field near the Price complaint well and RRC Test Hole #4 (fig. 3). Apparent conductivities in this area are about 10 mS/m (fig. 20h), similar to those measured along line A farther south. No elevated conductivities indicative of salinization were measured using either the 20- or 40-m coil separation, but exploration depths were insufficient to reach reported water depths of 83 m in this area. Conductivity slices from the airborne geophysical survey at depths of 10 to 50 m also show low apparent conductivities in this area; conductivities begin increasing at depths of 60 m and greater.

Line I is a 200-m-long line acquired using the 20-m coil separation farther downstream along Lacy Creek (fig. 3). Apparent conductivities along this line are about 30 mS/m (fig. 20i), slightly lower than those observed farther upstream along line B but higher than typical plateau conductivities. Values along this line are consistent with patterns of relatively high conductances at low elevations evident on the apparent conductance map (fig. 16) and with apparent conductivities displayed on the shallow depth slices (10- to 30-m depth) in this area (figs. A1 to A3).

EXTENT AND INTENSITY OF SALINIZATION

Airborne and ground-based geophysical data from Sterling County show that, in general, ground conductivity is relatively low across the area. This finding is consistent with the distribution and predominance of fresh to slightly saline water in the alluvial and Antlers aquifers. Although there has been significant oil and gas exploration and production in the area, particu-

larly in the Parochial Bade and Durham fields, the extent of salinization appears to be limited. Elevated conductivities consistent with shallow salinization that has impacted and might continue to impact the alluvial and Anters aquifers is present in the Parochial Bade field, particularly near the abandoned salt-water disposal pits mapped by Renfro (1993). Conductivities within the field, along the draw through the field, and on the northern perimeter of the field are relatively high compared to similar settings elsewhere in the survey area, suggesting that salinization related to oilfield development has occurred. The Durham Oil Field is surrounded by an area of relatively low conductivity that persists from depths as shallow as 20 m to as deep as 120 m. There is little or no evidence of shallow salinization in or near this field.

Conductivity images between about 40 and 90 m depth show an area of elevated apparent conductivity that extends about 3 km south of Lacy Creek toward the northeastern part of the Parochial Bade field (figs. A4 to A9). There is no water data from these depths in this area to determine whether the increased conductivity is related to increased water salinity or some other cause. Apparent conductivity within the common well-depth range in the valleys is relatively low, suggesting there has been no impact on the alluvial aquifer.

CONCLUSIONS

A high-resolution airborne geophysical survey covering 162 km² was completed west of Sterling City in late August and early September 2001. Magnetic field data acquired during the flights reveal accurate locations of most of the oil and gas wells within the survey area. In some cases, aerial photographic evidence demonstrates that the magnetic field anomalies are more accurate representations of well position than the plotted locations from the RRC database. Wells located nearly equidistant from the flight lines, which were spaced at 100 m, produce anomalies that can be missed by the airborne instruments. Depending on location relative to the flight lines, magnetic anomalies caused by wells spaced closer than the flight-line spacing can appear as a single anomaly.

EM data acquired during the airborne survey show that ground conductivities in the survey area are relatively low. These low conductivities in the shallow, water-bearing strata indicate that the water held by these strata have low TDS concentrations typical of the fresh to slightly saline values reported from most of the water wells in the area. There are local areas of elevated conductivity, particularly in and around the Parochial Bade Oil Field, that suggest the TDS values of groundwater have been increased locally by oilfield activities. Both airborne and ground-based geophysical surveys indicate that the sites of abandoned salt-water disposal pits have elevated conductivities indicative of salinization. Elevated conductivities are also found near some of the test holes drilled during the RRC investigation of a well contamination complaint in the early 1990s. Conductivities measured in the shallow subsurface in and near the Durham Oil Field are relatively low, suggesting little or no salinization associated with this field in the shallow subsurface.

ACKNOWLEDGMENTS

This project was funded by the Texas Water Development Board (TWDB) and Upper Colorado River Authority (UCRA) under contract number 2000-483-349. The Sterling County Underground Water Conservation District (SCUWCD) provided additional funds to Fugro Airborne Surveys to extend the survey area 5 km eastward. Project direction was provided by TWDB staff Edward Angle and UCRA staff Fred Teagarden. TWDB staff Brent Christian and SCUWCD staff Scott Holland and Bill Humble assisted with field studies. Airborne geophysical data were acquired and processed by Fugro Airborne Surveys staff Andrew Marshall, Leo Denner, Al Proulx, and Richard Williams and Voyageur Airways staff Bruce Waines, Steven Christeas, Nick Craig, and Brendon Fisher.

REFERENCES

- Eifler, G. K., Jr., and Barnes, V. E., 1974, San Angelo sheet: The University of Texas at Austin, Bureau of Economic Geology, Geologic Atlas of Texas, scale 1:250,000.
- Freeze, R. A., and Cherry, J. A., 1979, Groundwater: Englewood Cliffs, New Jersey, Prentice-Hall, Inc., 604 p.
- Frischknecht, F. C., Labson, V. F., Spies, B. R., and Anderson, W. L., 1991, Profiling using small sources, *in* Nabighian, M. N., ed., Electromagnetic methods in applied geophysics — applications, part A and part B: Tulsa, Society of Exploration Geophysicists, p. 105-270.
- Geonics Limited, 1992, Protem 47 operating manual: Mississauga, Ontario, variously paginated.
- Hefford, S., 2001, Airborne magnetic and MEGATEM II electromagnetic multicoil survey, San Angelo, Sterling County: Logistics and Processing Report, Fugro Airborne Surveys, not consecutively paginated.
- Kaufman, A. A., and Keller, G. V., 1983, Frequency and transient soundings: Elsevier, Amsterdam, Methods in Geochemistry and Geophysics, No. 16, 685 p.
- McNeill, J. D., 1980, Electromagnetic terrain conductivity measurement at low induction numbers: Mississauga, Ontario, Geonics Limited, Technical Note TN-6, 15 p.
- Paine, J. G., Dutton, A. R., and Blüm, M., 1999, Using airborne geophysics to identify salinization in West Texas: The University of Texas at Austin, Bureau of Economic Geology Report of Investigations No. 257, 69 p.
- Parasnis, D. S., 1973, Mining geophysics: Amsterdam, Elsevier, 395 p.
- Parasnis, D. S., 1986, Principles of applied geophysics: Chapman and Hall, 402 p.
- Renfro, W. C., 1993, Water well contamination investigation on the Price Ranch, Sterling County, Texas: Railroad Commission of Texas, 23 p.

Robinove, C. J., Langford, R. H., and Brookhart, J. W., 1958, Saline-water resources of North Dakota: U.S. Geological Survey, Water-Supply Paper 1428, 72 p.

Spies, B. R., and Frischknecht, F. C., 1991, Electromagnetic sounding: *in* Nabighian, M. N., ed., Electromagnetic methods in applied geophysics— applications, part A and part B: Tulsa, Society of Exploration Geophysicists, p. 285–386.

West, G. F., and Macnae, J. C., 1991, Physics of the electromagnetic induction exploration method, *in* Nabighian, M. N., ed., Electromagnetic methods in applied geophysics — applications, part A and part B: Tulsa, Society of Exploration Geophysicists, p. 5–45.

APPENDIX.

Conductivity-depth slices between 10 and 200-m depth

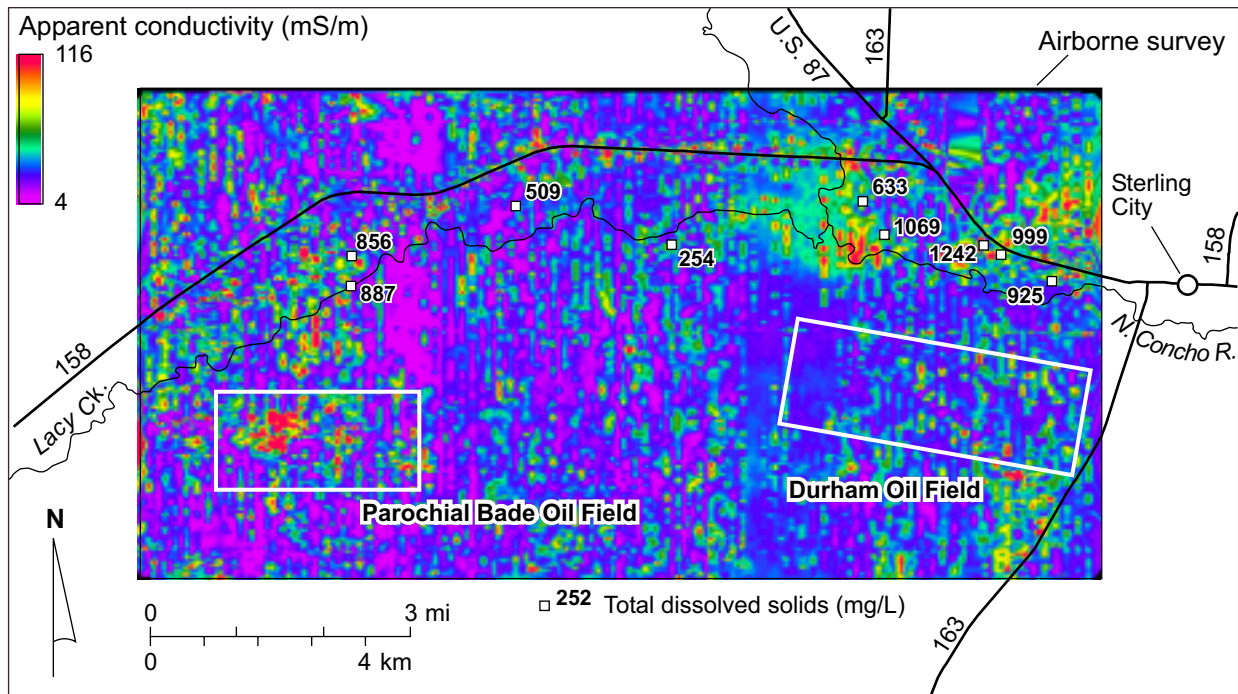


Figure A1. Apparent conductivity at a depth of 10 m. Also shown are locations of wells with TDS values from samples interpreted to be from this depth range.

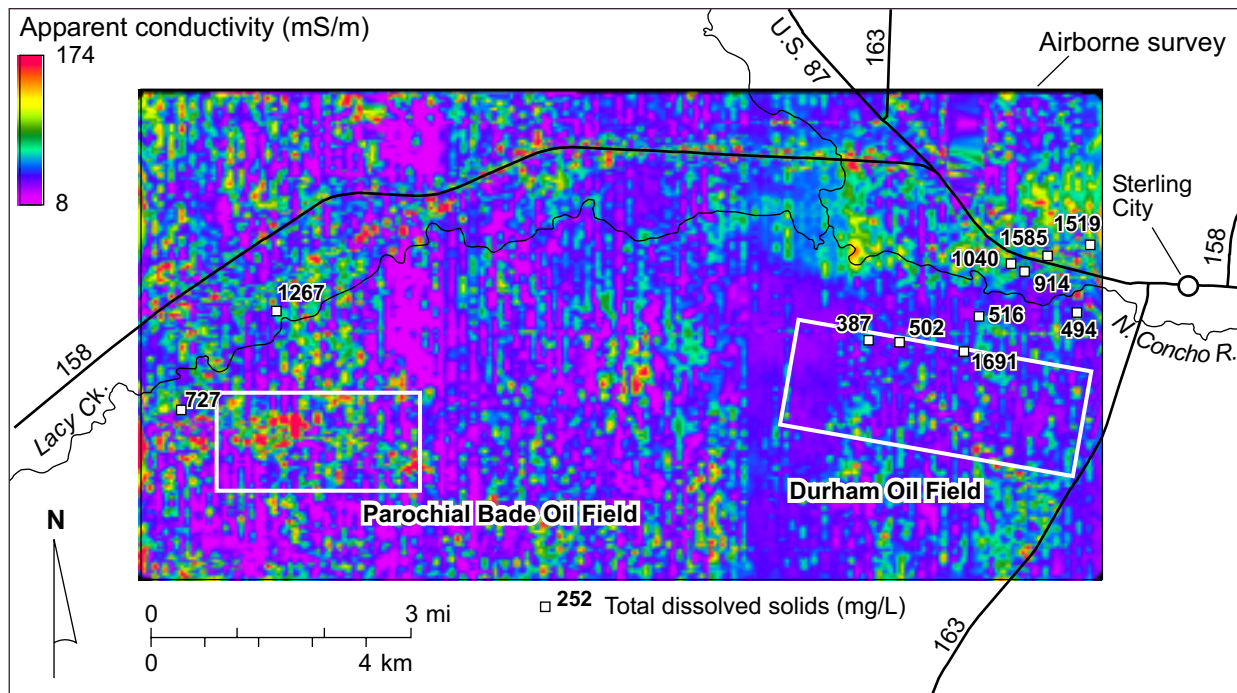


Figure A2. Apparent conductivity at a depth of 20 m. Also shown are locations of wells with TDS values from samples interpreted to be from this depth range.

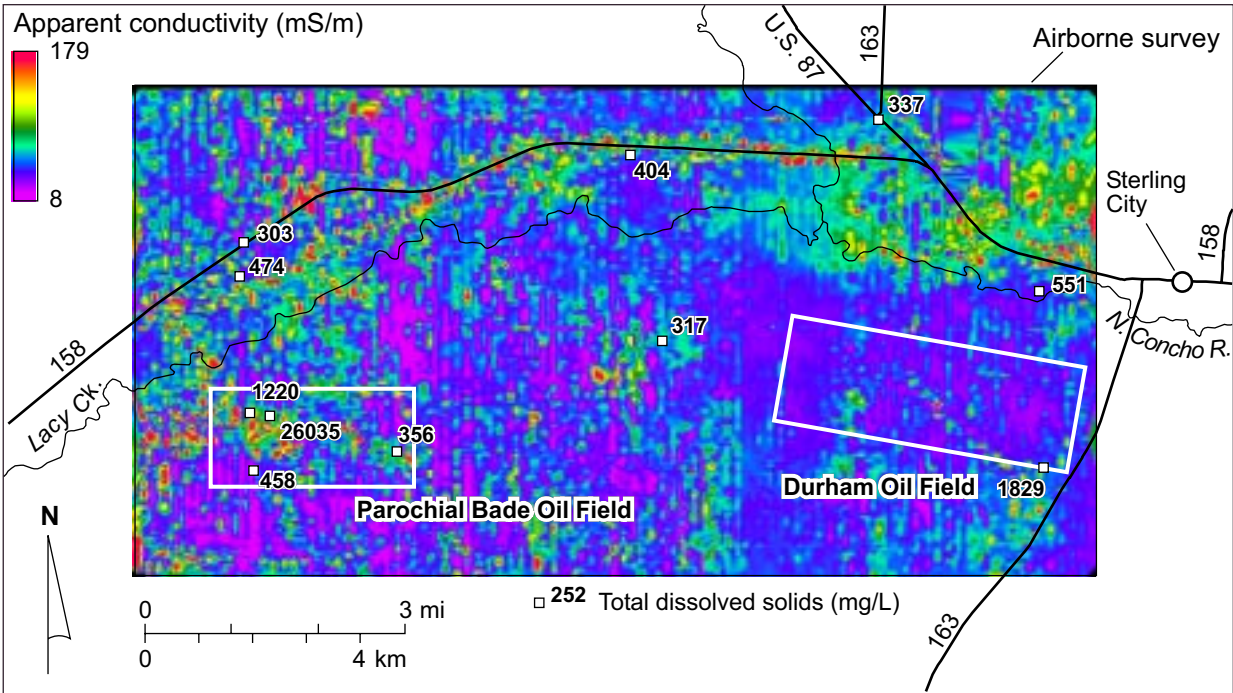


Figure A3. Apparent conductivity at a depth of 30 m. Also shown are locations of wells with TDS values from samples interpreted to be from this depth range.

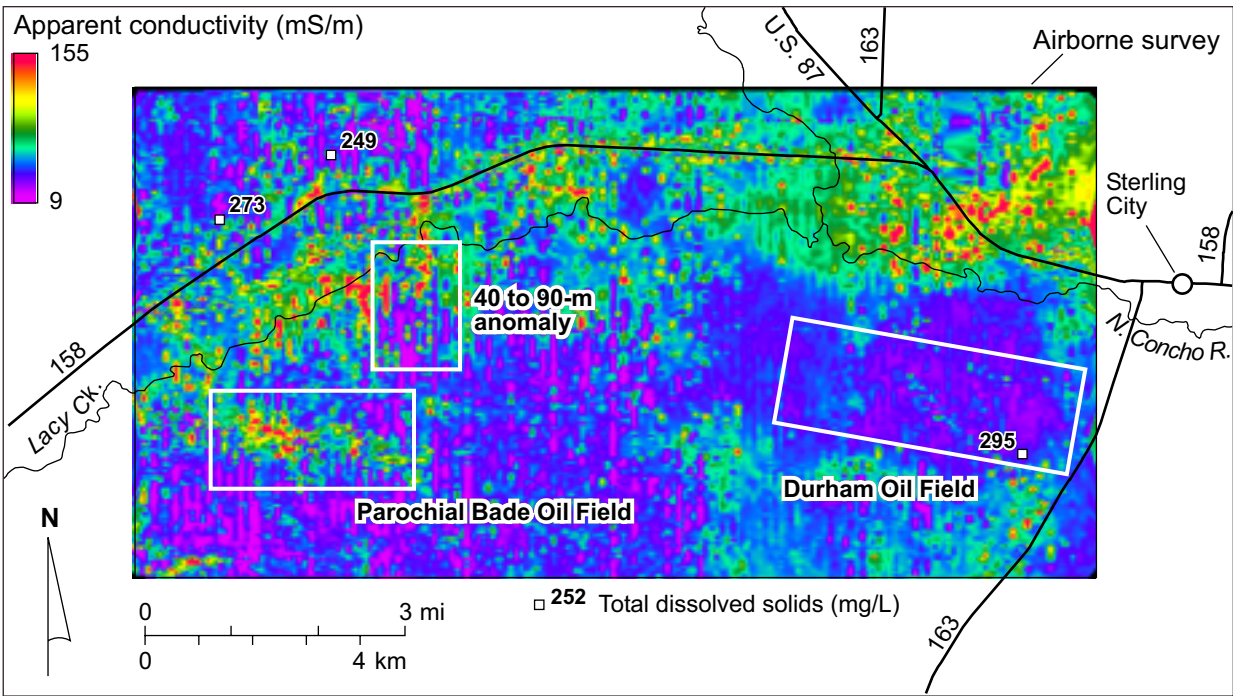


Figure A4. Apparent conductivity at a depth of 40 m. Also shown are locations of wells with TDS values from samples interpreted to be from this depth range.

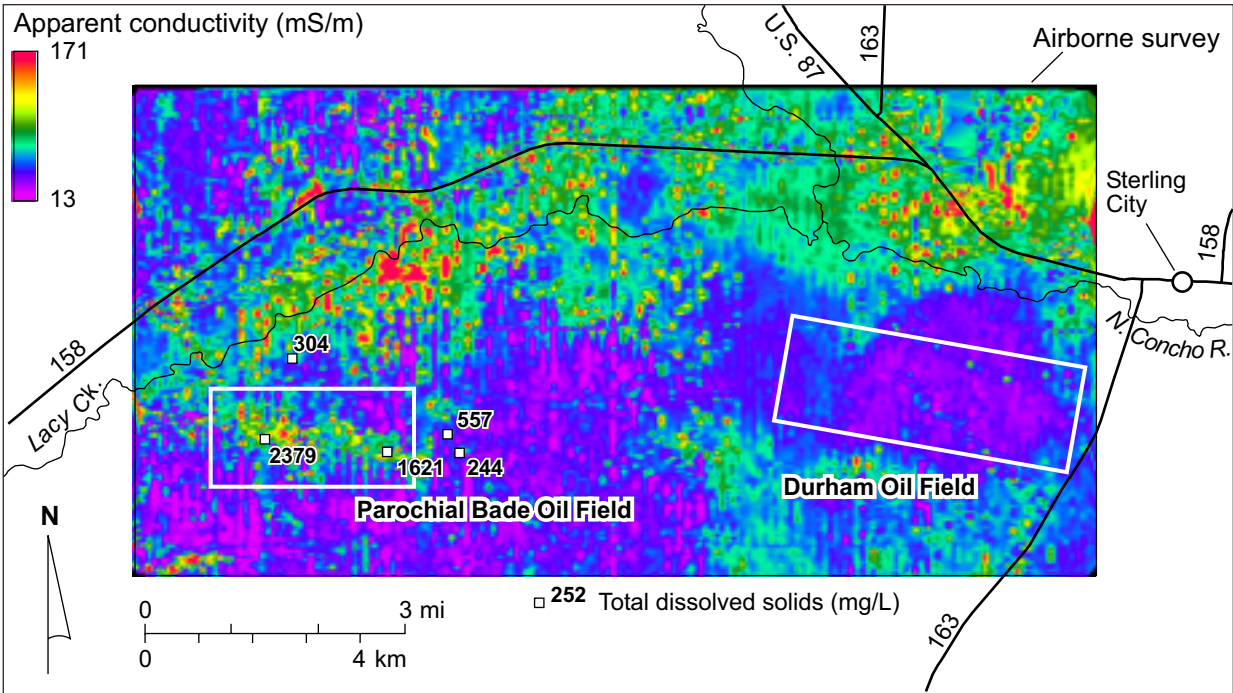


Figure A5. Apparent conductivity at a depth of 50 m. Also shown are locations of wells with TDS values from samples interpreted to be from this depth range.

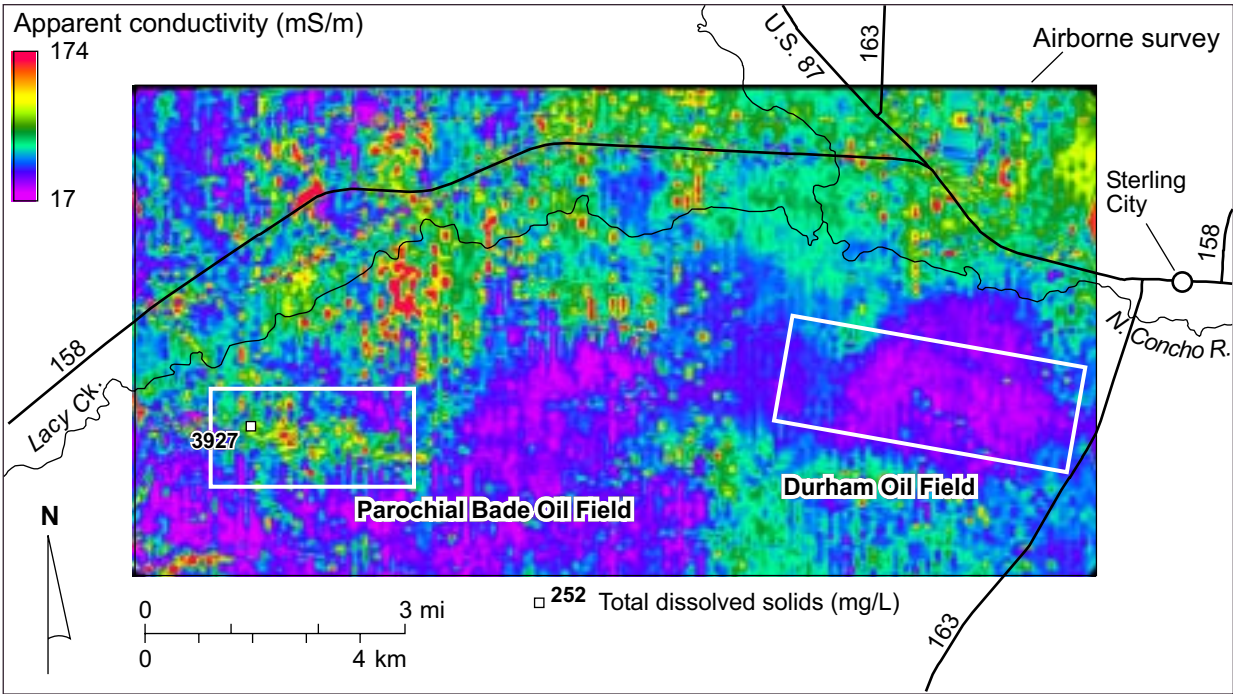


Figure A6. Apparent conductivity at a depth of 60 m. Also shown are locations of wells with TDS values from samples interpreted to be from this depth range.

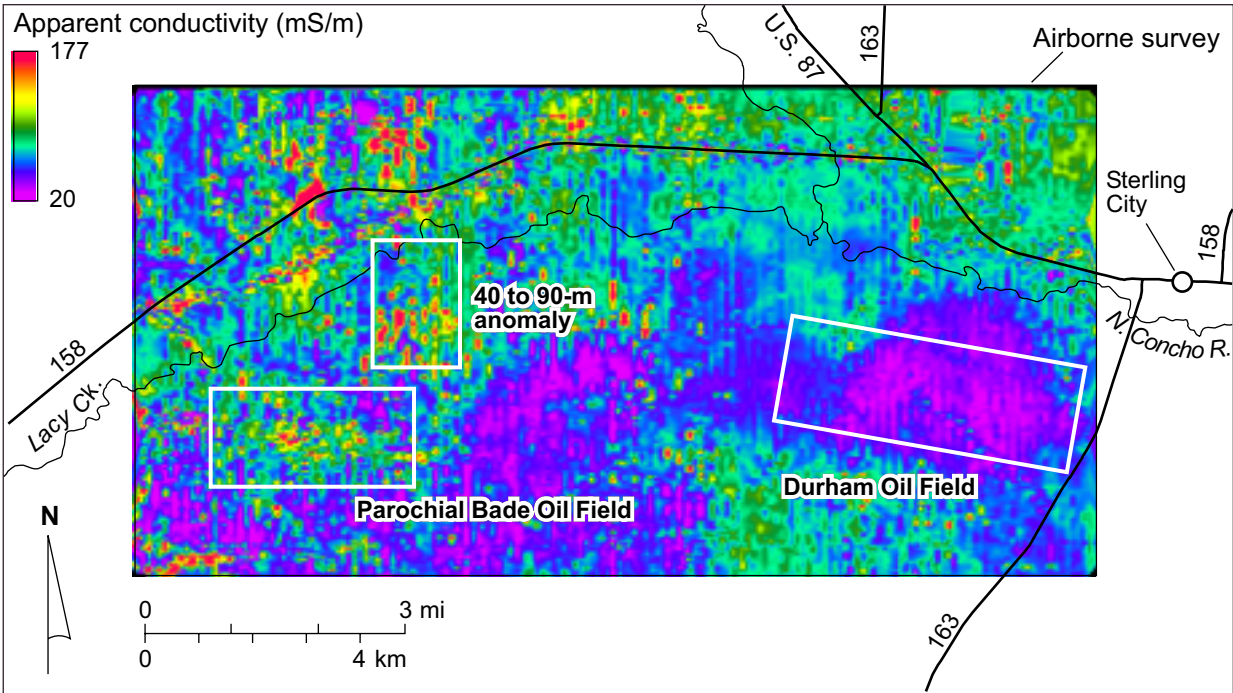


Figure A7. Apparent conductivity at a depth of 70 m.

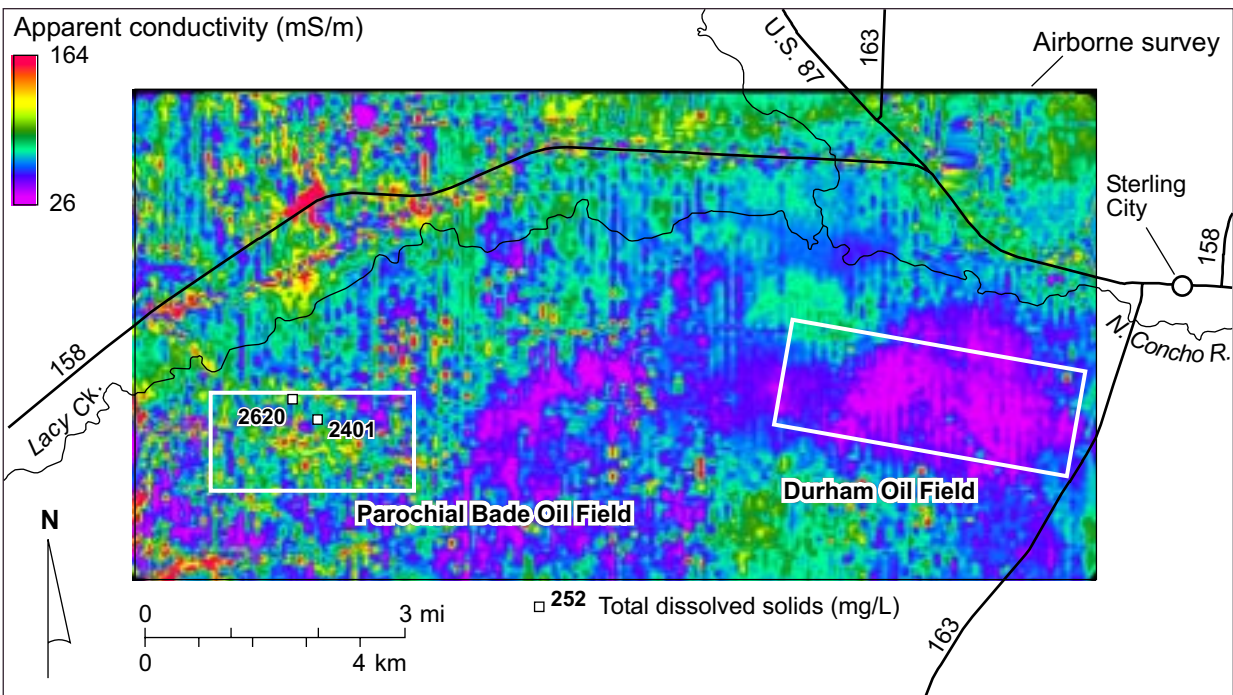


Figure A8. Apparent conductivity at a depth of 80 m. Also shown are locations of wells with TDS values from samples interpreted to be from this depth range.

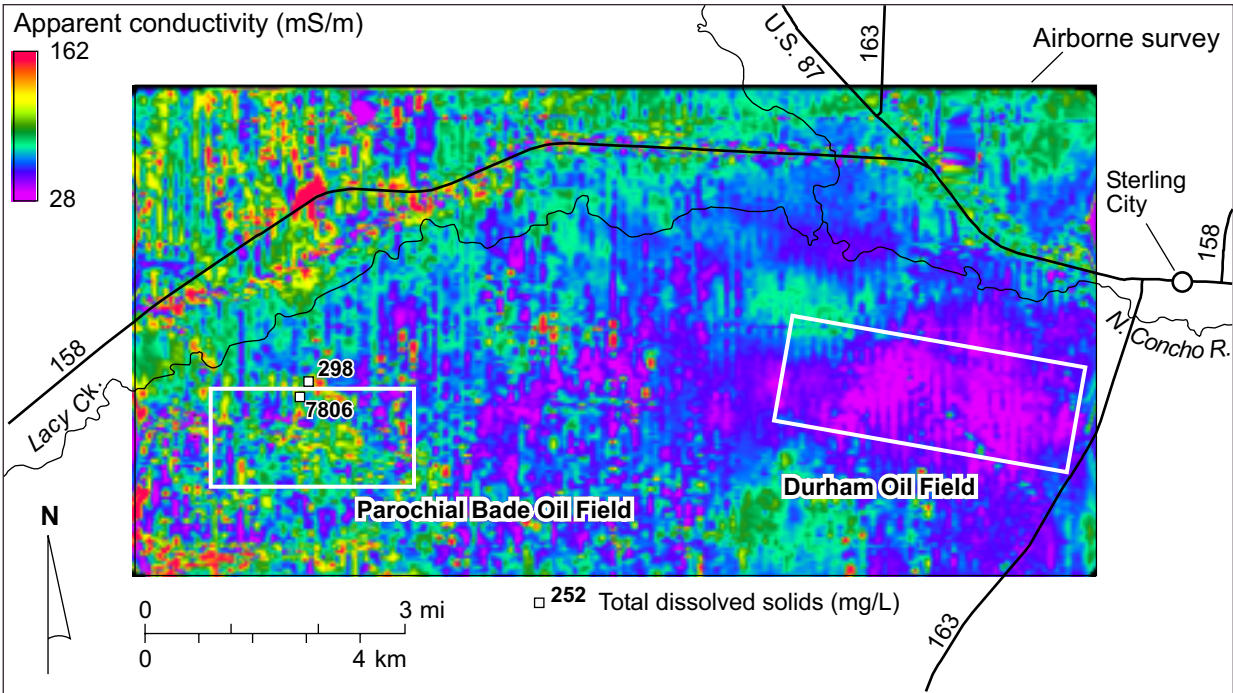


Figure A9. Apparent conductivity at a depth of 90 m. Also shown are locations of wells with TDS values from samples interpreted to be from this depth range.

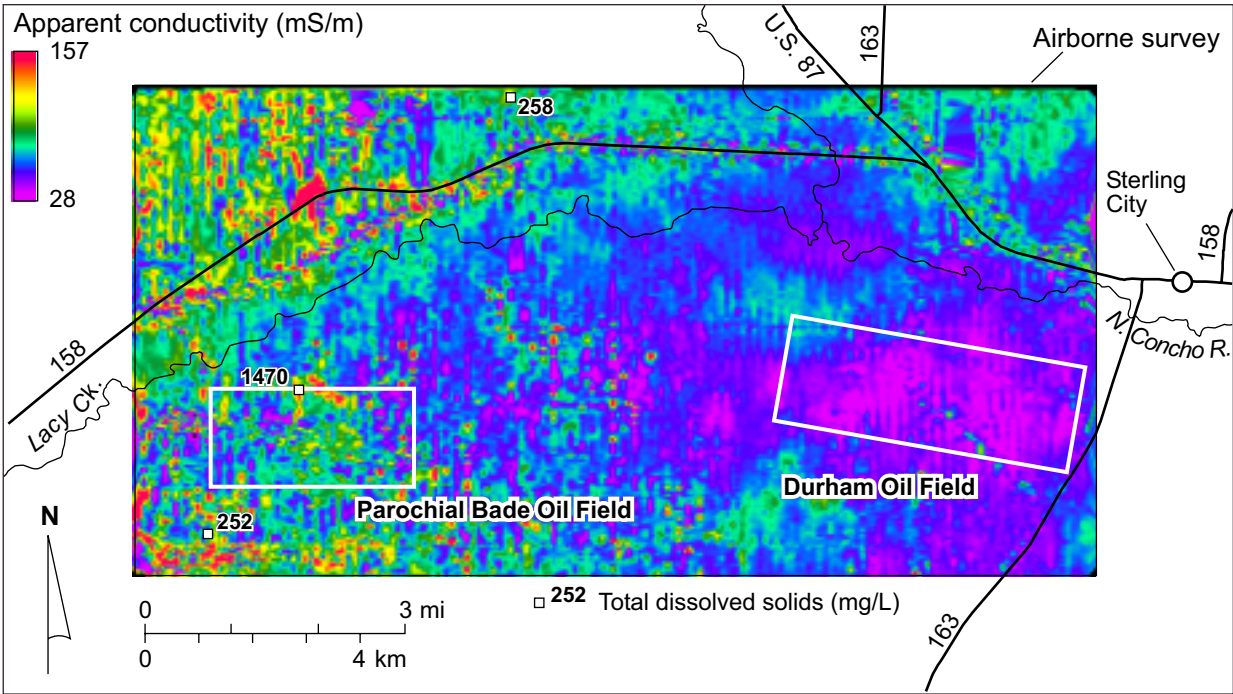


Figure A10. Apparent conductivity at a depth of 100 m. Also shown are locations of wells with TDS values from samples interpreted to be from this depth range.

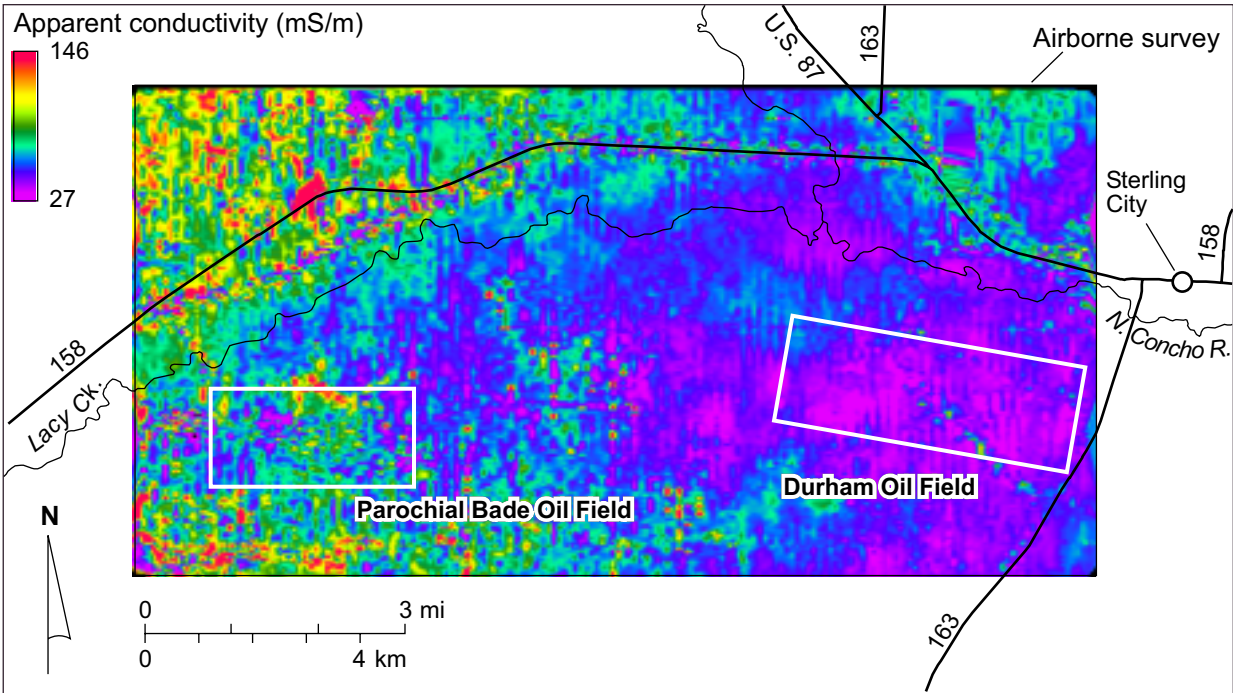


Figure A11. Apparent conductivity at a depth of 110 m.

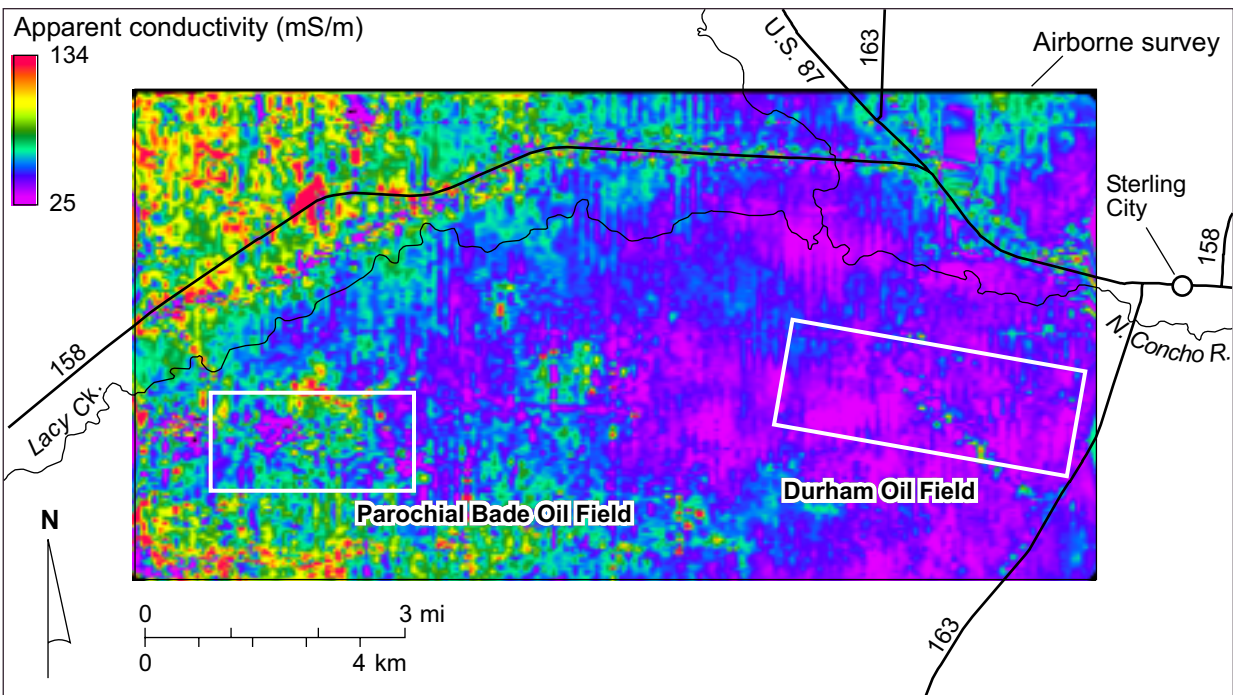


Figure A12. Apparent conductivity at a depth of 120 m.

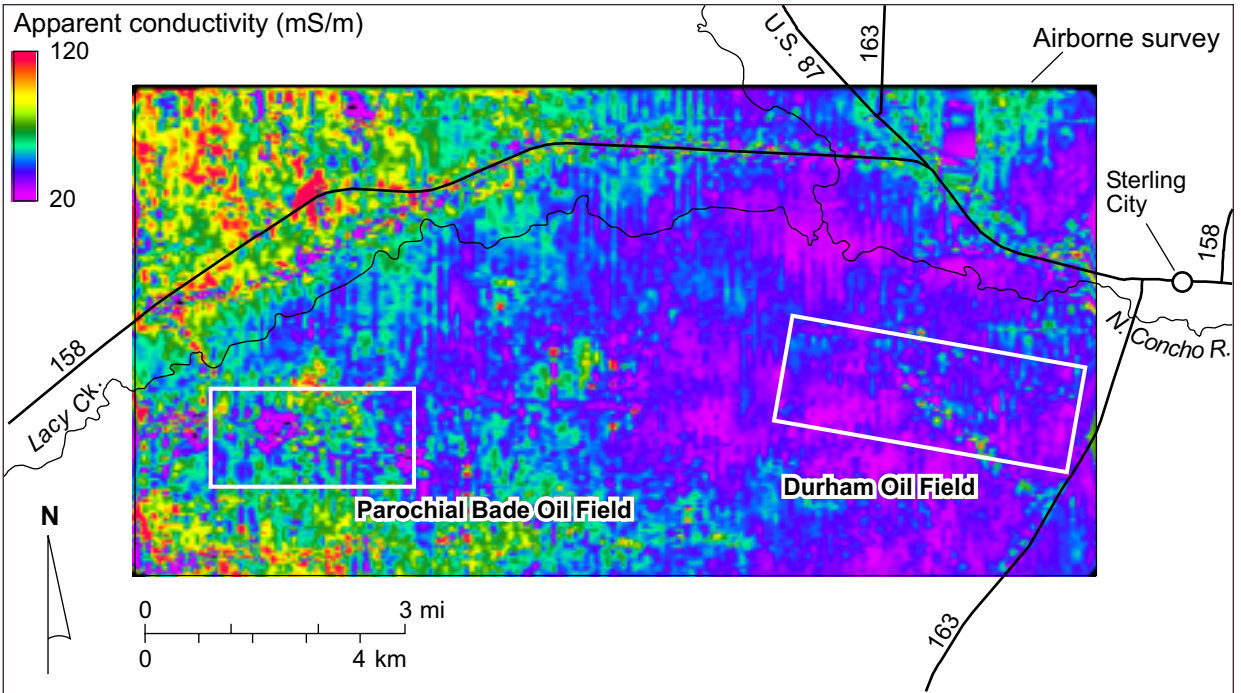


Figure A13. Apparent conductivity at a depth of 130 m.

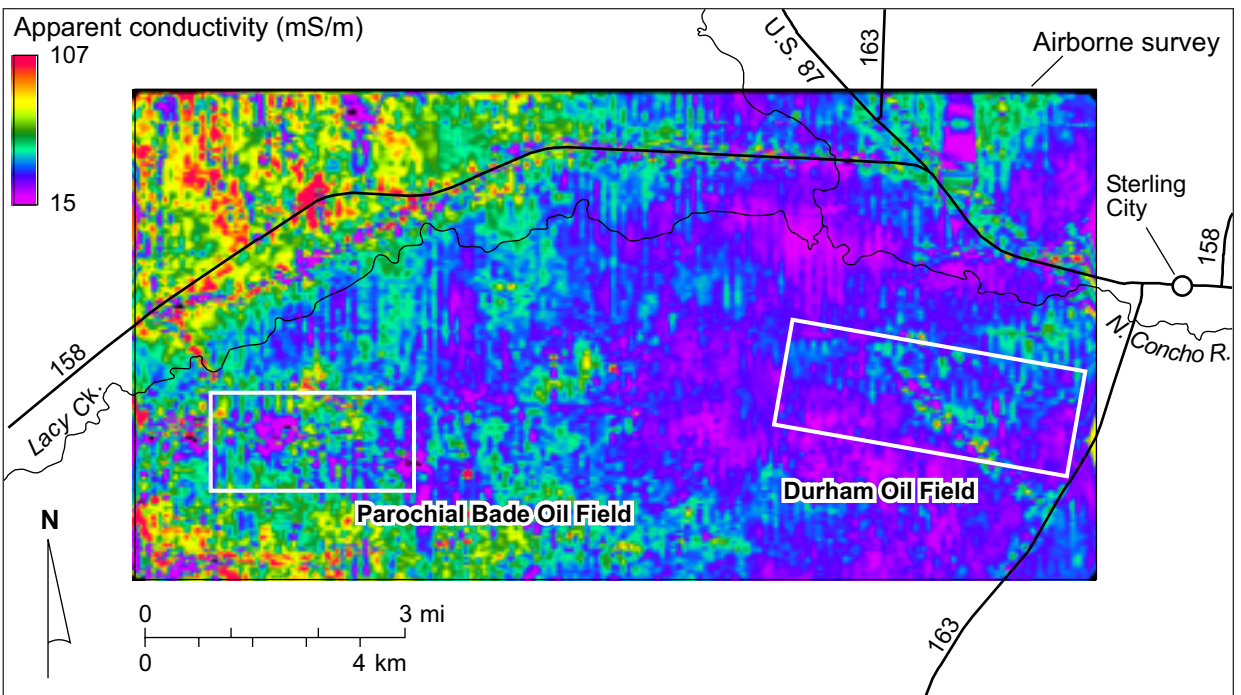


Figure A14. Apparent conductivity at a depth of 140 m.

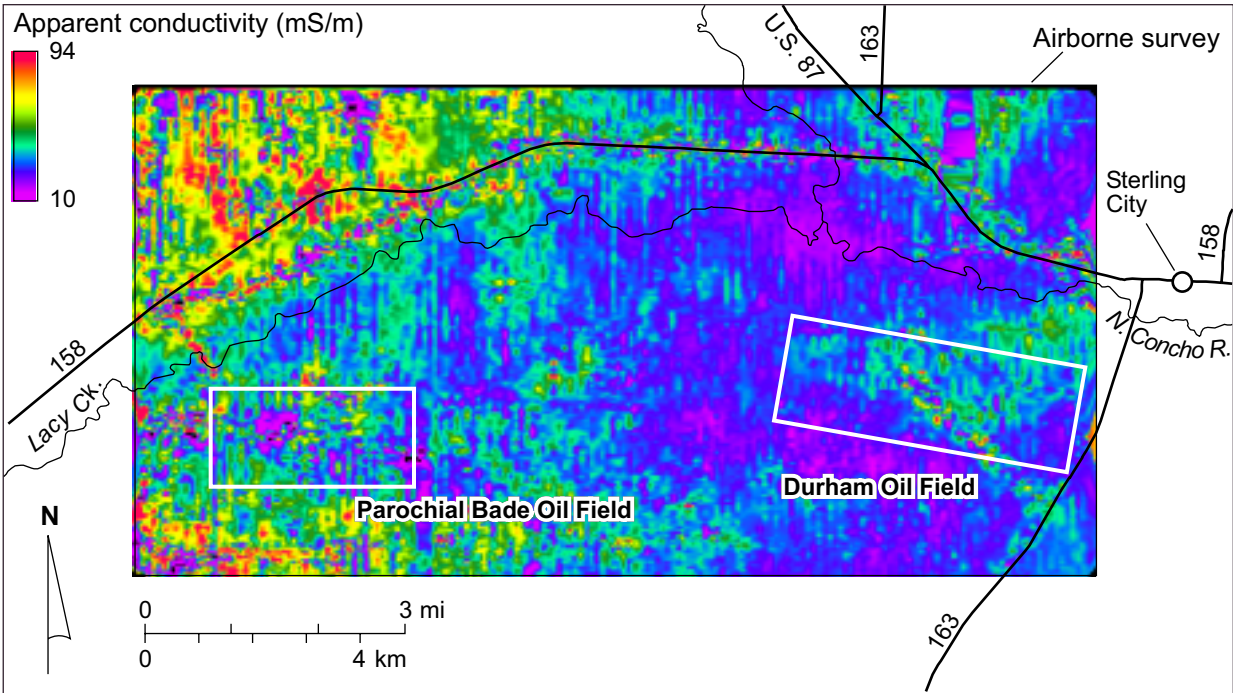


Figure A15. Apparent conductivity at a depth of 150 m.

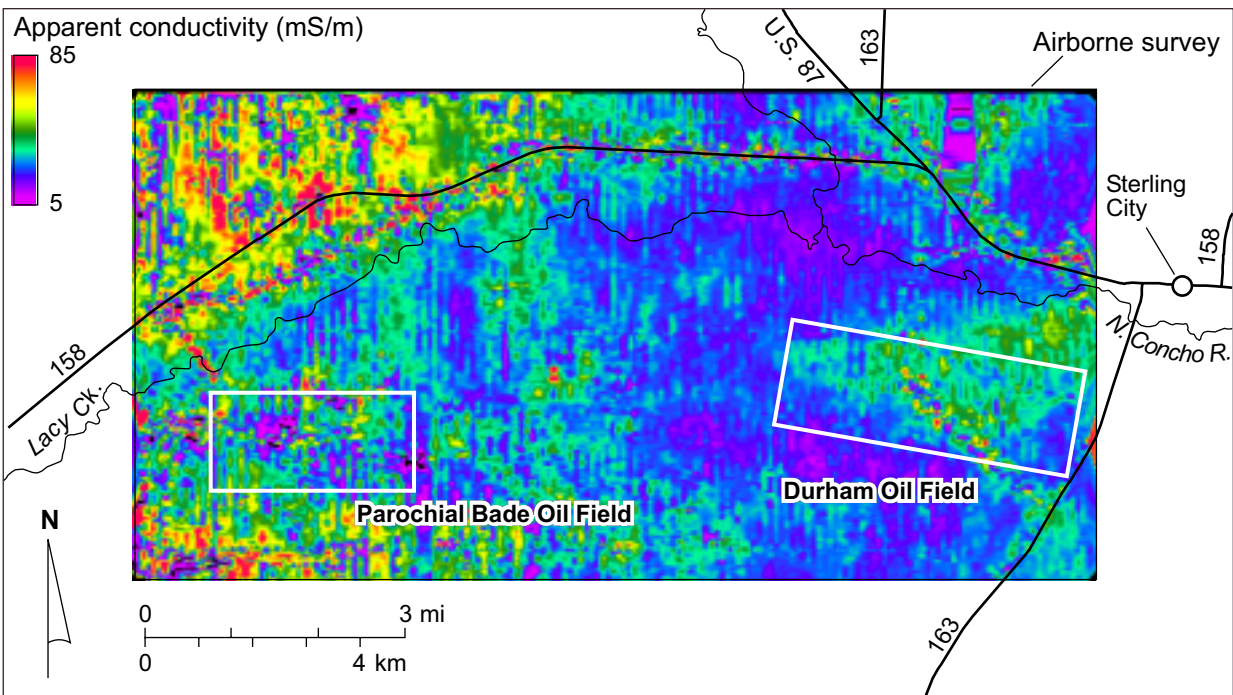


Figure A16. Apparent conductivity at a depth of 160 m.

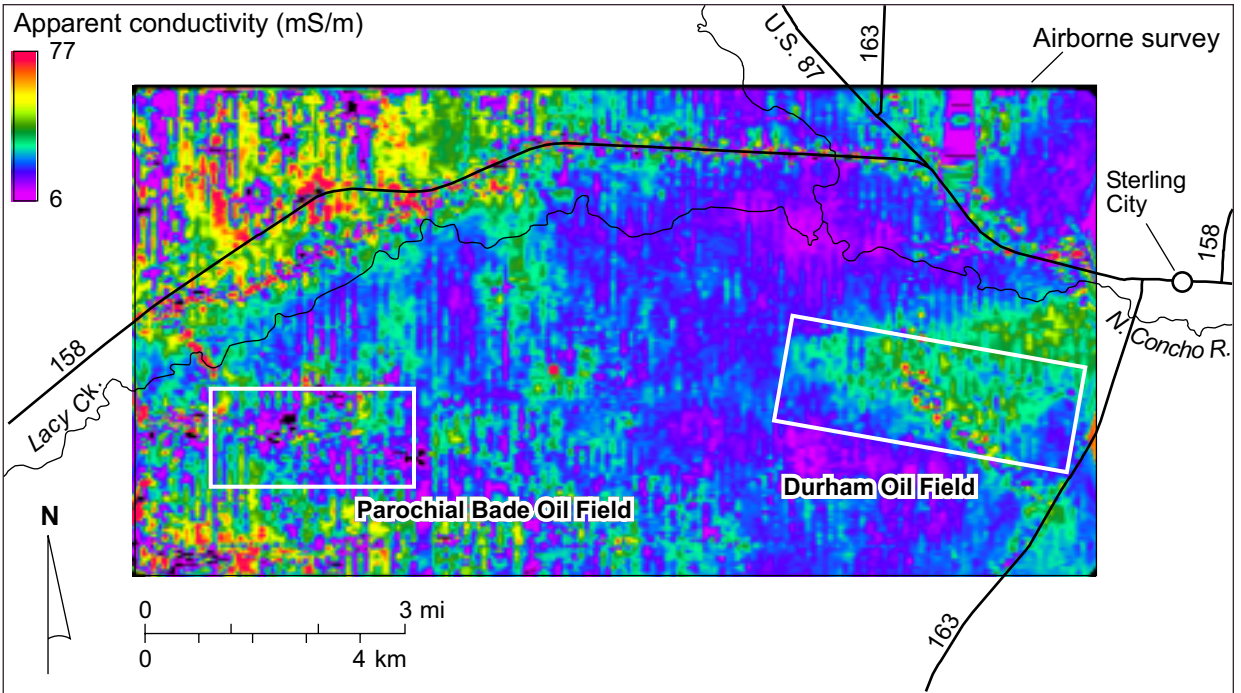


Figure A17. Apparent conductivity at a depth of 170 m.

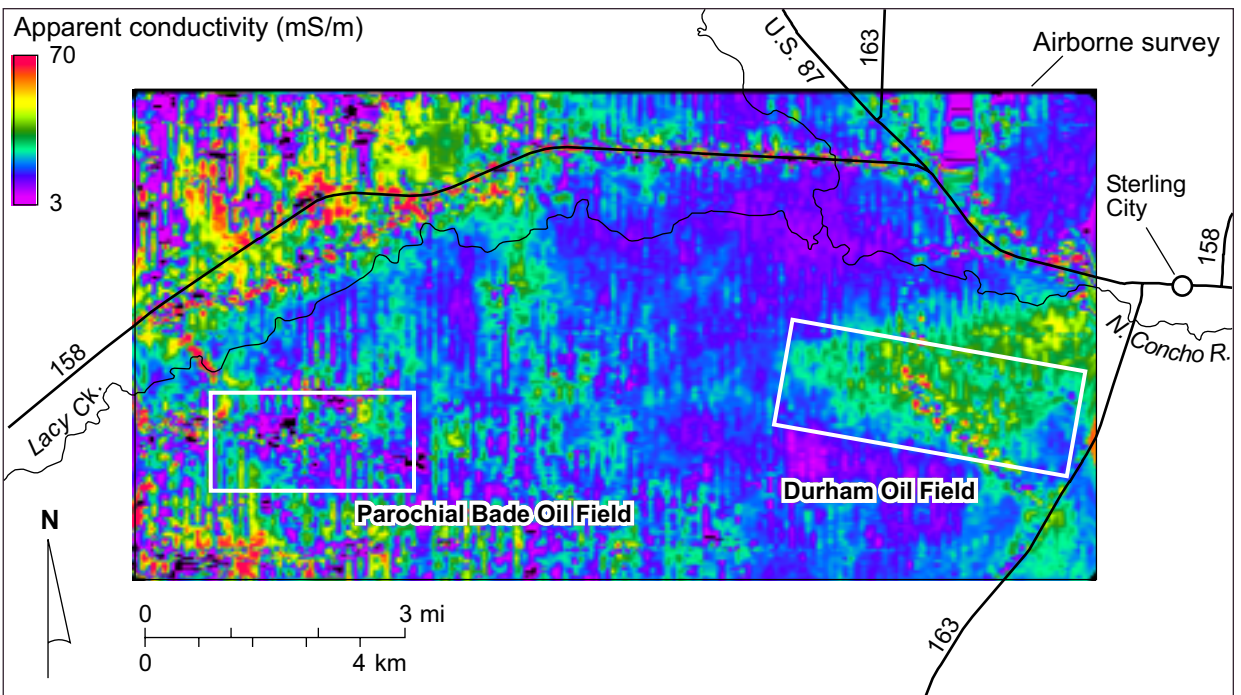


Figure A18. Apparent conductivity at a depth of 180 m.

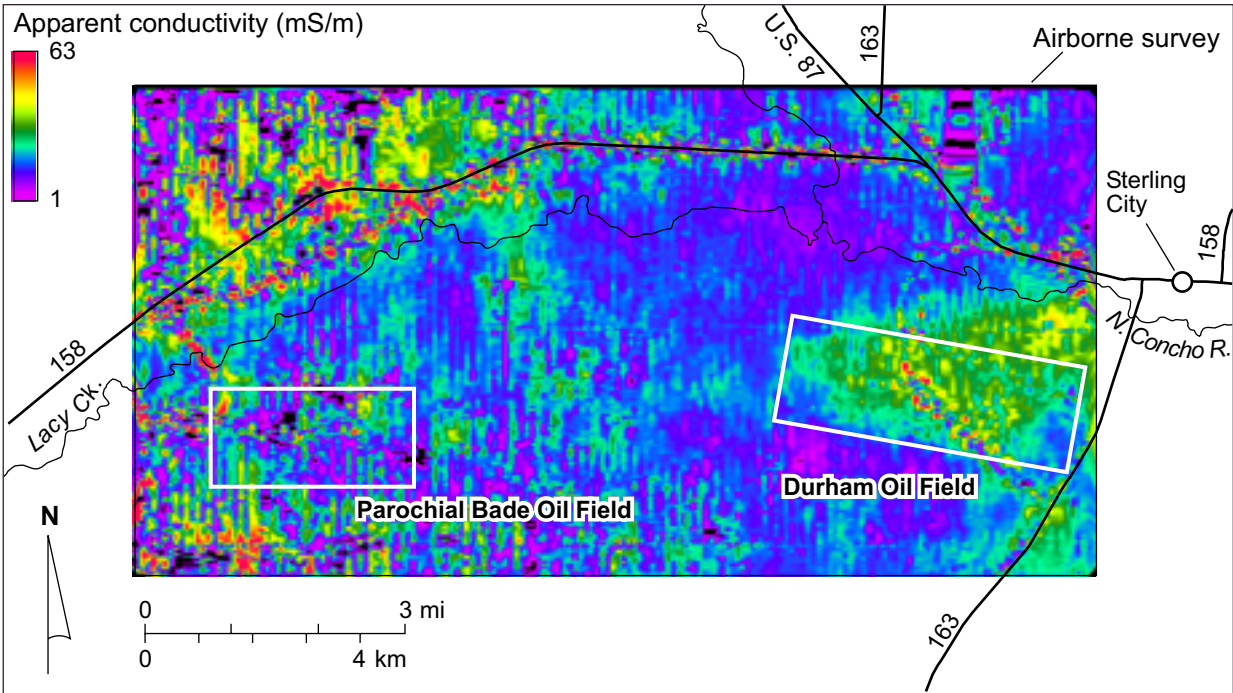


Figure A19. Apparent conductivity at a depth of 190 m.

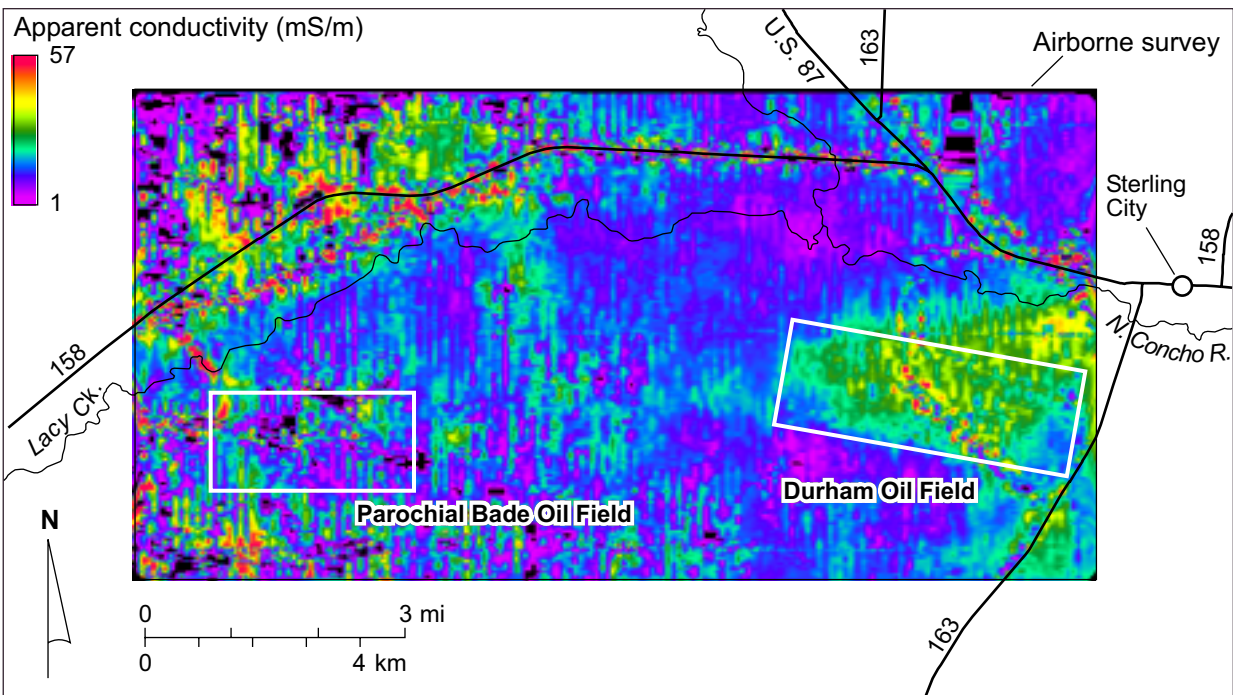


Figure A20. Apparent conductivity at a depth of 200 m.